Order Number 1349474

# Measurement of saturated hydraulic conductivity with a sealed double ring infiltrometer at Page Ranch, Arizona

Johnejack, Kent Robert, M.S.

The University of Arizona, 1992

U·M·I
300 N. Zeeb Rd.
Ann Arbor, MI 48106

# MEASUREMENT OF SATURATED HYDRAULIC CONDUCTIVITY WITH A SEALED DOUBLE RING INFILTROMETER AT PAGE PANCH, ARIZONA

by

Kent Robert Johnejack

---

A Thesis Submitted to the Faculty of the

DEPARTMENT OF HYDROLOGY AND WATER RESOURCES

In Partial Fulfillment of the Requirements
For the Degree of

MASTER OF SCIENCE
WITH A MAJOR IN HYDROLOGY

in the Graduate College

THE UNIVERSITY OF ARIZONA

1 9 9 2

THE UNIVERSITY OF ARIZONA
GRADUATE COLLEGE

As members of the Final Examination Committee, we certify that have read the thesis prepared by Kent R. Johnejack entitled Measurement of Saturated Hydraulic Conductivity with a Sealed Double Ring Infiltrometer at Page Ranch, Arizona

and recommend that it be accepted as fulfilling the thesis requirement for the Degree of Master of Science

| | |
|---|---|
| Michael J. Sully | Date 7/13/92 |
| L. Gray Wilson | Date 7/13/92 |
| Randy Bassett | Date 7/20/92 |
| | Date |

Final approval and acceptance of this thesis is contingent upon the candidate's submission of the final copy of the dissertation to the Graduate College.

I hereby certify that I have read this thesis prepared under my direction and recommend that it be accepted as fulfilling the thesis requirement.

Thesis Director Michael J. Sully Date 7/13/92

**STATEMENT BY AUTHOR**

This thesis has been submitted in partial fulfillment of requirements for an advanced degree at The University of Arizona and is deposited in the University Library to be made availaboratoryle to borrowers under rules of the Library.

Brief quotations from this thesis are allowable without special permission, provided that accurate acknowledgment of source is made. Requests for permission for extended quotation from or reproduction of this manuscript in whole or in part may be granted by the head of the major department or the Dean of the Graduate College when in his or her judgment the proposed use of the material is in the interests of scholarship. In all other instances, however, permission must be obtained from the author.

SIGNED: Kent R Dhuyack

**APPROVAL BY THESIS DIRECTOR**

This thesis has been approved on the date shown below:

Michael J. Sully
Assistant Professor of
Hydrology and Water Resources

7/13/92
Date

**ACKNOWLEDGMENTS**

The author would like to thank Dr. Michael Sully for all his help on this thesis, as well as Dr. L.G. Wilson and Dr. Randy Bassett for their service as committee members. In addition, this project would not have been possible without the support of the Risk Management Department at the University of Arizona, who provided all the materials and supplies. Especially, thanks are due to Lloyd Wundrock at the Risk Management Department who acted as project manager. Last but not least, thanks are given to Daniel B. Stephens and Associates (Albuquerque) for performing some of the laboratory work.

## TABLE OF CONTENTS

## TABLE OF CONTENTS (continued)

## LIST OF FIGURES

# LIST OF TABLES

## ABSTRACT

A sealed double ring infiltrometer (SDRI) was used at Page Ranch, Arizona to measure saturated hydraulic conductivity ($K_{sat}$) in a test clay pad, as well as to characterize preferential flow and transport mechanisms. $K_{sat}$ varied from $3.5x10^{-9}$ to $2.2x10^{-10}$ cm/sec depending on treatment of matric potential at the wetting front. These in-situ $K_{sat}$ values were about one order of magnitude less than the laboratory values that ranged from $10^{-7}$ to $10^{-9}$ cm/sec. Although the pad was not instrumented to detect a shallow wetting front, the dye front and water content data indicated that flow penetrated 4 to 6 cm by the end of the 75 day test. Tracer data suggested that bromide moved to 18 or 20 cm by diffusion and that the effective diffusion coefficient was 15 to $21x10^{-10}$ $m^2$/sec. Preferential flow, as judged by the uniformity of the dye front and bromide tracer movement, was insignificant.

# CHAPTER 1

# INTRODUCTION

## Background

Because of increasing concern over groundwater contamination from hazardous and radioactive waste sites, compacted clay liners and/or caps were required at all sites beginning in the early 1980's. Evidence accumulated by the mid-1980's suggested that laboratory tests of saturated hydraulic conductivity often yielded results several orders of magnitude less than those from in-situ tests or measured leakage. The U.S. Environmental Protection Agency (EPA), as a result of the Resource Conservation and Recovery Act (U.S. Federal Register, 1987), now requires that all soil liners and caps meet a minimum saturated hydraulic conductivity of $1 \times 10^{-7}$ cm/sec that is verified by in-situ tests.

Beginning in 1962, the University of Arizona disposed of its hazardous and low level radioactive waste at Page Ranch near Oracle, Arizona. This site has been closed since 1984, but because wastes were placed in unlined pits, concern has continued over possible groundwater contamination. The Arizona State Department of Environmental Quality (ADEQ) has

mandated closure of the site, which includes construction of a compacted clay cover to prevent infiltration into the wastes.

Prior to construction of a full-scale liner or cap, a test section is usually constructed to insure that the clay, as well as the construction methods, can produce a liner or cap that meets the minimum standard for saturated hydraulic conductivity. Geotechnical parameters such as optimum moisture content, relative compaction, soil density, method and amount of compaction, and height of lifts are often specified from the results of the test section.

As part of this mandated closure, the Risk Management Department (University of Arizona) requested the help of the Department of Hydrology and Water Resources to measure the saturated hydraulic conductivity of a test clay cap using a sealed double ring infiltrometer (SDRI). Environmental Engineering Consultants, Inc. of Tucson, Arizona authored the closure plan and provided oversight on the SDRI test, as well as for the entire closure project. ADEQ has regulatory jurisdiction over the project.

The SDRI project was initiated in January, 1991 by Dr. Michael Sully and the Vadose Zone Monitoring Class (Hydrology 508). SDRI test plans were prepared by the class and approved by Risk Management, Environmental Engineering Consultants, Inc., and ADEQ. Because the project start was delayed until May, 1991, further class participation was limited to setting up the SDRI.

## Overview of the SDRI

A variety of field methods can be used to measure in-situ saturated hydraulic conductivity, including single or double ring infiltrometers, disc permeameters, borehole tests, porous probes, and air-entry permeameters,. The sealed double ring infiltrometer (SDRI) has emerged as the preferred instrument because of its ability to accurately measure very low infiltration rates. It was developed in the mid-1980's in order to overcome the shortcomings of other in-situ and laboratory tests, and is now marketed by Trautwein Soil Testing Equipment of Houston, Texas.

The largest source of error in both laboratory and in-situ tests is the small sample volume which can exclude paths of preferential flow or zones of variable compaction. With a 25 square foot inner ring, the SDRI samples a much larger volume

than any other method. The double ring design promotes one-dimensional flow in the inner ring, and assures that only vertical flow is measured instead of a combination of horizontal and vertical flow.

The SDRI has several features that adapt it to low permeability materials. The sealed inner ring is essential for measuring infiltration rates that may be less than the evaporation rate. Measuring infiltration rates by a drop in water surface elevation, which would be imperceptible with low permeability materials, is replaced by measuring the mass flow rate from a flexible bag to the nearest gram (or less if desired). Furthermore, including a swell gage with the SDRI allows for correction of infiltration rates for water taken up during swelling. Tracers can also be added to evaluate preferential flow.

## Scope and Purpose

The practical purpose of this study was to accurately measure the saturated hydraulic conductivity of the test clay cover in order to obtain approval for the full scale cover from ADEQ. The research or academic purposes were more involved:

- to identify the depth and pattern of the wetting front using physical measurements, such as water content, and tracer methods such as bromide and dye.

- to compare in-situ and laboratory measurements of saturated hydraulic conductivity.

- to evaluate preferential flow paths or zones of variable compaction.

- to evaluate transport by advective flow and diffusion.

- to evaluate the ability of the unsaturated flow code PICARD to predict the observed cumulative infiltration and wetting front position.

- to suggest new or revised SDRI procedures.

Although laboratory work and computer modelling were part of this investigation, it was primarily a field study. The effects of construction methods, test pad size or geometry, or type of clay on hydraulic conductivity were not studied, nor were different in-situ testing methods or tracers compared. Construction inspection and documentation were handled by the

consultant, as were all geotechnical and laboratory hydraulic conductivity testing. Mixed English and SI units were used throughout this thesis because although the scientific community uses SI units, the engineering community in the United States still relies on English units.

# CHAPTER 2

## LITERATURE REVIEWED

This chapter is divided into three sections: 1) comparison of laboratory and in-situ measurement of saturated hydraulic conductivity, 2) identification of a wetting front in compacted clay, and 3) the roles of advection and diffusion in the transport of conservative tracers in compacted clay. None of these sections are intended to provide an exhaustive literature review of the hydrologic behavior of compacted clay; rather, they are brief reviews of selected papers that are pertinent to this SDRI study.

The review of the literature concerning laboratory and in-situ $K_{sat}$ measurements proceeds in chronological order from the early 1980's to show the evolution of published methods on permeability testing leading to development of the SDRI. The second section focuses on a qualitative understanding of dye and anionic tracer movement that can be used to approximately locate a wetting front. Finally, transport by advection and diffusion in compacted clay were compared with particular emphasis on published accounts of bromide diffusion and bromide diffusion coefficients.

## Laboratory vs. In-Situ Measurement of $K_{sat}$

Daniel (1981) published the first of many papers on the behavior of compacted clay. The hydraulic conductivity of two sizes of undisturbed cores (3.8 cm and 6.4 cm diameters) were measured in the laboratory with one larger sample (243.8 cm diameter) tested in the field. The small cores yielded $K_{sat}$ of $1x10^{-7}$ and $8x10^{-9}$ cm/sec, respectively, whereas the large sample had a $K_{sat}$ of $3x10^{-5}$ cm/sec; the actual $K_{sat}$ as back-calculated from leakage rates based on a water balance, was $1x10^{-5}$ cm/sec. Daniel concluded that sample size is significant in predicting hydraulic conductivity.

Four case histories of compacted clay liners (Daniel, 1984) showed that field $K_{sat}$, as back-calculated from measured leakage rates, was 5 to 100,000 times greater than predicted by laboratory values of $K_{sat}$. Leakage rates were estimated by water balance and/or water level changes in monitoring wells. All liners were thin (0.2 m to 0.6 m), had little or no quality control during construction, and were subject to desiccation before use. Unrepresentative samples for laboratory testing, whether recompacted or undisturbed cores, were seen as the major source of error.

A 1984 EPA review paper (U.S. EPA, 1984) summarized the state of permeability testing for low permeability materials by identifying a number of differences between laboratory and field conditions as possible sources of error in laboratory testing:

- water content during compaction
- amount and type of compactive effort
- size of clay aggregates
- presence of deleterious substances (roots,debris, etc.)
- entrapped air
- temperature of permeant
- chemical composition of permeant
- hydraulic gradient (i.e., high gradients in laboratory tests)
- alteration during sampling, trimming, and transporting of samples
- sample size

The EPA report further concluded that: 1) all laboratory methods suffer from small sample size and/or disruption of samples when transported or remixed, 2) it was not possible at that time to distinguish between variation caused by laboratory testing methods and spatial variation of the materials themselves, and 3) determination of hydraulic conductivity was the limiting factor to further development of transport models for low permeability materials.

The emphasis in the literature then changed from recognition of the problem to studies specifically designed to quantify variation in testing methods, and variation inherent in the materials. Small test liners and field-scale liners, usually

with underdrain systems, were used to compare laboratory and in-situ measurements to values derived from actual leakage rates.

Day and Daniel (1985) constructed two small prototype liners with underdrains in order to compare a variety of laboratory and in-situ measurements of $K_{sat}$ to the actual $K_{sat}$ back-calculated from leakage rates. Each 6-inch liner was constructed with a different type of clay but both were contained in a pit 20 feet wide by 50 feet long. Laboratory tests used three types of permeameters on recompacted and undisturbed cores; laboratory tests underpredicted $K_{sat}$ by an average factor of 1000. Small diameter single ring infiltrometers (22 inch and 48 inch diameters) and double ring infiltrometers (12 inch diameter inner ring, 20 inch diameter outer ring) yielded values within 1.2 times of the actual $K_{sat}$. The authors concluded laboratory methods were flawed by their small sample size, and that greater emphasis should be placed on field permeability testing. In the resulting journal discussions many authors criticized laboratory testing methods that were very different from field conditions, and thus could account for differences between laboratory and in-situ $K_{sat}$. In particular, excessive hydraulic gradients in laboratory tests, different compaction water contents, and different

types and amount of compactive effort were cited (Bagchi, 1986; Dakessian, and Lewis, 1986; Pacey and Scharlin, 1986).

Rogowski (1986) conducted tests on a field-scale facility designed specifically to investigate spatial variability of hydraulic conductivity. A 30 foot by 75 foot by 1 foot thick clay pad with underdrains was subjected to a 9 month ponding test with infiltration rates measured at 250 points on the pad. Density changes and swelling were also measured at each of the 250 points. The spatial distribution of $K_{sat}$ ranged from $10^{-5}$ to $10^{-8}$ cm/sec but was not correlated to the distribution of density or shrinking/swelling. Laboratory permeability was $10^{-8}$ cm/sec as measured by a falling head test on a recompacted sample. The spatial variability in $K_{sat}$ of three orders of magnitude was attributed to preferential flow in zones of lower compaction density.

Because of the small sample size issue, as well as recognition that evaporation rates may be greater than infiltration rates when dealing with compacted clay, Trautwein developed the sealed-double ring infiltrometer (SDRI) in the mid-1980's. Its first use was documented by Daniel and Trautwein (1986) which described an SDRI test on a landfill cover. Infiltration rates declined over the two month test, and the

final $K_{sat}$ value was $8x10^{-8}$ cm/sec. Laboratory tests with a flexible wall permeameter and back pressure yielded values of $K_{sat}$ from $1x10^{-7}$ to $3x10^{-9}$ cm/sec. Suction head in the compacted clay was not considered in the calculations of the in-situ hydraulic conductivity.

Daniel (1989) continued his examination of measurement of hydraulic conductivity with a comparison of in-situ tests for compacted clay. According to Daniel, the double ring design promoted one dimensional flow from the inner ring and minimized temperature fluctuations, the sealed inner ring eliminated evaporation, and the five foot diameter of the inner provided a large sample size. The long testing period (weeks to months) was seen as the main disadvantage. The author criticized in-situ tests in general because they do not insure complete saturation of the material, and unsaturated soils are less permeable than saturated soils.

The U.S. EPA sponsored a research project by Elsbury, et al. (1990) to construct and test a clay liner. Four SDRIs were installed in a 1 foot thick pad along with a large pan lysimeter in order to compare in-situ $K_{sat}$ to a variety of

laboratory measurements of $K_{sat}$. The $K_{sat}$ values of $1x10^{-4}$ to $3x10^{-5}$ cm/sec from the SDRIs fell within the range of $K_{sat}$ from the laboratory tests ($10^{-3}$ to $10^{-9}$ cm/sec), but failed to meet the $10^{-7}$ cm/sec federal standard. The $K_{sat}$ of about $10^{-4}$ cm/sec from the lysimeter was also higher than the federal standard. The authors concluded that unless laboratory samples are prepared and tested according to the same procedures as field construction, laboratory results can seriously deviate from in-situ results. The pad became fully saturated and outflow was established, thus eliminating suction head at the wetting front as a variable in the hydraulic gradient calculations.

Panno et al. (1991) monitored infiltration into a 0.9 m thick pad for two years as part of another EPA sponsored project. Among other instrumentation, four SDRIs were used to characterize infiltration; the resulting values of $K_{sat}$ varied from 2.5 to $2.9x10^{-9}$ cm/sec. Based on tensiometer and water balance data, the predicted depth of the wetting front was 26 and 44 cm after one and two years, respectively, and $K_{sat}$ was $4.2x10^{-8}$ cm/sec from two years of data. The authors concluded that it was possible to build a liner that meets federal standard.

## Identification of the Wetting Front

A wetting front can be detected by a variety of physical, visual, and chemical means. Physical methods include changes in water content, dielectric constant, and wet density, as well as consistency changes from hard to soft. Visual means may include dyes, but can be as simple as a change from dark to light soil. Chemical means are based on tracers, both dye and solutes. The test clay pad for this thesis project was not instrumented to physically detect a shallow wetting front, and therefore this literature discussion will focus on the use of tracers to approximately locate a wetting front.

Dyes vary greatly in their tendency to sorb to soil, but most are strongly retarded with respect to the wetting front. Corey (1968) found that Acid-Red 1 was the most mobile among the anionic dyes tested, but none of the anionic dyes moved as rapidly as water. Ghodrati and Jury (1990) found that in a loamy sand Acid-Red 1 was retarded with respect to a conservative tracer ($Cl^-$) and that Dispersed-Orange 3 dye penetrated to a minimal depth of a few centimeters; both dyes moved behind the wetting front. In an agricultural soil in Arizona, Hussen (1992) showed that a dye solution advanced more in some parts of the soil profile than others, but in all cases was behind the uniform wetting front.

Cationic dyes are usually sorbed from solution and therefore are often used to stain preferential flow pathways. Elsbury et al. (1990) found that compacted clay removed a 0.1% solution of methylene blue dye from solution before it even reached the first lift interface at about six inches. As part of a proposed study of clay liners at Weldon Spring, Missouri, laboratory tests showed that FD&C Green #3 stained clay and could be rinsed off only partially with 0.01 $CaCl_2$ (DBS&A, 1991). The $N^+$ functional group of FD&C Green #3 was possibly attracted to the negatively charged clay surfaces. Although neither of these studies compared the movement of cationic dyes to the wetting front, clearly the implication is that they would be strongly retarded.

Conservative anionic tracers, such as $Cl^-$ and $Br^-$, are poorly sorbed and move with the wetting front. Bowman (1984) claimed that bromide was not sorbed by a silty clay loam even though the figures showed that peak outflow concentration of bromide was only about 80% of the input concentration. Hills et al. (1991) used a retardation factor of 0.84 for bromide at the Las Cruces Trench Experiment, indicating that the bromide front moved slightly faster than the wetting front. The retardation factor is defined as the ratio of the average

linear pore water velocity to the velocity of the $C/C_o=0.5$ point on the concentration profile of the retarded constituent (Freeze and Cherry, 1979).

When soil grains, and in particular clay particles, are so close together that the solution in the pores is made up of only double layers, anions will be excluded from the pore water (Drever, 1988). Such anionic exclusion allows the passage of water but not anions, and thus anion movement will be relegated to the larger pores where double layers occupy a smaller portion of the pore space. Anions should therefore travel with the fastest moving part of a wetting front.

In summary, both anionic and cationic dyes are retarded with respect to a wetting front, but because cationic dyes can react with the clay faction, they are retarded more than anionic dyes and follow well behind the wetting front. On the other hand, conservative tracers such as $Cl^-$ and $Br^-$ travel with the wetting front with a velocity slightly faster than the average linear velocity. This qualitative understanding of dye and anionic tracers can be used to approximately locate a wetting front.

## Transport in Compacted Clay

Compacted clay, with its high bulk density, low permeability, and potential for shrinking and swelling, is a very different material than other porous media. A quote from Shackelford (1991b) illustrates the relative roles of advection and diffusion in transport in compacted clay:

> "In the absence of coupled flow processes, the best barrier is one in which diffusion controls the transport."

Rowe (1987) described and quantified the relative roles of advection and dispersion in compacted clay. Transport by advection is solely a function of seepage velocity, whereas dispersion, defined as a combination of mechanical dispersion and diffusion, is a function of seepage velocity and diffusion. Rowe stated that mechanical dispersion is insignificant compared to diffusion when the seepage velocity is less than 0.1 m/yr ($3.28 \times 10^{-7}$ cm/sec). In most practical situations involving clay barriers Rowe further asserted that $K_{sat}$ would be less than $10^{-7}$ cm/sec, hydraulic gradients would be less than 0.2, and diffusion would dominate because the resulting advective velocities would be less than 0.006 m/yr.

Shackelford et al. (1989) suggested that diffusion was the dominant transport mechanism when the seepage velocity is on the order of $1.6 \times 10^{-8}$ cm/sec (which would be the case in a clay liner if the hydraulic gradient was one, the porosity 0.5, and the hydraulic conductivity $8 \times 10^{-9}$ cm/sec). The author further asserted that because clay liners are required to have a hydraulic conductivity less than $10^{-7}$ cm/sec, diffusion was expected to be a significant, if not dominant, transport mechanism.

Fick's first and second laws are universally used by researchers for steady state and transient diffusion modelling, respectively (Rowe, 1987; Rowe et al., 1988; Quigley et al., 1987; Johnson et al., 1989; Shackelford et al., 1989; Shackelford, 1991; Shackelford and Daniel, 1991a and 1991b). Both equations require that $D_o$, the free solution (aqueous) diffusion coefficient, be known a priori in order to calculate diffusion rates.

Solutes diffuse more slowly in porous media than in free solution because solids occupy some of the cross sectional area for diffusion, and the pathways for diffusion are more tortuous (Shackelford and Daniel, 1991a). Tortuosity can not be measured directly and therefore is lumped together with $D_o$

to make a new parameter termed the effective diffusion coefficient or $D^*$. Porosity ($\eta$) is usually included as a separate term for the cross sectional area available to the diffusing solute.

Diffusion in unsaturated soils is subject to an additional decrease in cross sectional area of flow relative to saturated conditions. In this case, volumetric water content ($\theta$) is simply substituted for porosity ($\eta$) (Rowe, 1987; Rowe et al., 1988; Quigley et al., 1987; Johnson et al., 1989; Shackelford et al., 1989; Shackelford, 1991; Shackelford and Daniel, 1991a and 1991b).

Published values of $D_o$ and $D^*$ were needed for data analysis because this thesis project used bromide as a tracer. Shackelford and Daniel (1991a) list a $D_o$ of $20.8 \times 10^{-10}$ $m^2$/sec (at 25 °C) for $Br^-$; Quigley et al. (1987) graphically showed a similar value for $Br^-$ of about $21 \times 10^{-10}$ $m^2$/sec at 25 °C.

Values of $D^*$ for $Br^-$ diffusion in commercially available kaolinite and Lufkin clay (a naturally occurring smectite) were determined by two methods by Shackelford et al. (1989). By measuring decreasing concentrations in a reservoir above a clay sample, average $D^*$ values of $7.2 \times 10^{-10}$ and $18.2 \times 10^{-10}$ $m^2$/sec

were estimated for kaolinite and Lufkin clay, respectively. Fitting theoretical diffusion curves to measured concentration-depth profiles in a sample yielded a $D^*$ of $5.8 \times 10^{-10}$ $m^2$/sec for the kaolinite. A curve could not be fit to the concentration-depth profile in the Lufkin clay. The authors noted that the $D^*$ values of 3.7 to $7.0 \times 10^{-10}$ $m^2$/sec found by Barraclough and Tinker (1981,1982) for $Br^-$ in soil matched their results in kaolinite closely. They also noted that their $D^*$ value of $18.2 \times 10^{-10}$ $m^2$/sec for $Br^-$ in Lufkin clay was much higher than any other published value.

Few field studies of anion diffusion have been conducted and as far as this author can determine none of them have used bromide as a tracer. Chloride, however, has a similar $D^*$ as bromide ($20.3 \times 10^{-10}$ $m^2$/sec). For example, Johnson et al. (1989) investigated waste chloride diffusion in natural clay beneath a landfill in Ontario and found that chloride reached a maximum depth of 83 cm in 5 years. Although this study has no direct relevance to the test pad at Page Ranch, it did illustrate the importance of diffusion in clay.

In summary, diffusion can be a significant, if not dominant, transport mechanism in compacted clay. Fick's first and second laws are usually used to quantify diffusion, and the

amount of diffusion depends on the degree of saturation and the effective diffusion coefficient ($D^*$). $D^*$ modifies the free solution diffusion coefficient ($D_o$) by lumping together a variety of factors including tortuosity and anion exclusion. Although a few studies have documented $D^*$ values for bromide in compacted clay, the results are tentative and vary greatly by type of clay.

# CHAPTER 3

# PROCEDURES

Although this project was primarily a field study, considerable laboratory work was involved, as well a some computer modelling. Therefore this chapter covers a wide range of procedures from the installation, operation, and removal of the SDRI, to soil extractions, ion chromatography, and geotechnical tests. Simulation of water content profiles is discussed in Chapter 6.

This chapter is not intended to be a detailed instruction manual for SDRI projects; rather, it summarizes pertinent procedures so that the strengths and weaknesses of the test can be evaluated. For the interested reader, several manuals and guides are listed in the references.

## Sequence of the SDRI Test

All field work and most laboratory work took place in 1991 as shown below:

| | |
|---|---|
| preparation of test plans | January-April, 1991 |
| test pad construction | April 15-22, 1991 |
| SDRI installation | April 22-24, 1991 |
| SDRI test/data collection | April 24-July 9, 1991 |
| SDRI removal/data collection | July 9-11, 1991 |
| soil solution extractions | August-December, 1991 |
| bromide tracer analysis | February-April, 1992 |
| computer modelling | April-May, 1992 |

## Setting Up the SDRI

Test Pad Construction

The test pad was located in an easily accessible area near the east fence line of the hazardous waste site at Page Ranch. Construction began on April 17, 1991 and was finished on April 22, 1991; a local contractor constructed the pad under the supervision of Environmental Engineering Consultants, Inc.

The pad was approximately 25 feet by 25 feet with 2H:1V side slopes, and the top of the pad was level to less than 4 inches on 12 feet. Pad thickness varied from 2.0 to 2.5 feet because of the slight slope of the existing ground.

Standard Proctor density tests indicated an optimum moisture content of 21.4% for maximum density, but this proved too wet to be workable by a vibratory sheepsfoot roller. Best workability occurred at a moisture content of 12 to 16% with a curing time of 16-24 hours before placement. The lifts of 8 to 12 inches were compacted with the rubber tires of an endloader, and a vibratory sheepsfoot compactor was used on the surface of a lift to insure bonding with the next lift. At the end of each construction day, the pad was soaked with water and covered with two layers of 7 mm thick black plastic.

The final surface of the pad was constructed by adding a thin lift (approximately 1 inch) and smoothing with a steel wheel roller. The pad was covered between construction and installation of the SDRI to prevent drying or cracking, and no personnel were allowed on the surface prior to SDRI installation. No fractures were visible in the finished surface.

Installation of Outer Ring

After assembling the 12 foot by 12 foot outer ring, it was placed on the test pad in order to scribe its location for digging the trenches. Care was taken to square the sides of the outer ring, and plywood was placed on the area where the inner ring would later be installed in order to prevent damage to the surface of the pad.

A trenching machine (Ditch Witch) with a 4 inch cutting bar was used to cut a 4 inch wide by 16 inch deep trench; a 2x4 was staked outside the outer ring to act as a guide for the tires of the Ditch Witch. The bottom of the trench was levelled to within 1 inch using brick hammers.

Volclay grout was mixed in a mortar mixer at the proportion of 17.5 gallons of water to one 50 pound bag of grout; this ratio had been previously determined by mixing trial batches

of grout at different ratios. Grout was placed to within 1 inch of the top of the trench with a wheelbarrow, and a piece of plywood acted as a splash guard to prevent splattering of the grout on the surface of the pad.

The outer ring was then pushed into the grout-filled trench with care taken to prevent any grout from running out onto the surface of the pad. While the grout was still soft, the outer ring was levelled with a carpenters level. Material excavated from the trench was mounded about a foot high around the outside of the outer ring to provide support for the walls of the outer ring. The inner surface of the pad was covered for the night with black plastic and the grout was left to set up over night before beginning the installation of the inner ring.

A plastic ruler was glued to the inside wall of the outer ring in order to later measure the depth of ponded water. It was offset 1-1/2 inches from the surface of the pad so that, for example, an actual depth of 12 inches would read as 10-1/2 inches.

Figure 3.1, SDRI Layout (located after the section on Tensiometer Installation), shows the configuration of the outer ring.

Installation of Inner Ring

Installation of the fiberglass inner ring (5 foot by 5 foot) began by scribing its location in the approximate center of the outer ring. A 2 inch wide by 4 inch deep trench was cut with brick hammers, and the bottom of the trench was levelled. As with the installation of the outer ring, protective plywood was placed over all surfaces not being trenched to prevent damage.

Grout was again mixed in a mortar mixer, and was placed in the trenches to within 1/2 inch of the top using a five gallon bucket and plywood as a splashguard. Prior to placing the inner ring, the surface of the inner ring was thoroughly cleaned to remove any debris or spilled grout. The inner ring was then pushed into the grout-filled trench until it rested on the bottom of the trench. Accurate levelling was not necessary as the fiberglass inner ring was formed with a slope towards its inlet/outlet ports.

Figure 3.1, SDRI Layout (located after the section on Tensiometer Installation), shows the configuration of the inner ring.

Tensiometer Installation

After installing the inner ring, six tensiometers were installed in the area between the inner and outer rings. Their approximate location, as well as the general layout of the SDRI, is shown in Figure 3.1. All tensiometers were Irrometer Moisture Indicators manufactured by Irrometer Company of Riverside, California.

Three tensiometers were installed 13-1/8 inches deep and the other three were installed 17-1/8 inches deep. Holes were dug with a 2-3/4 inch diameter hand auger with the final 2-1/4 inches of the hole were drilled with an electric drill and 7/8 inch bit. After pushing a tensiometer into a hole, a mixture of Volclay grout and clay cuttings were repacked into the hole. At this point the area between the inner and outer rings was recovered with black plastic to await the filling of the rings on the following day.

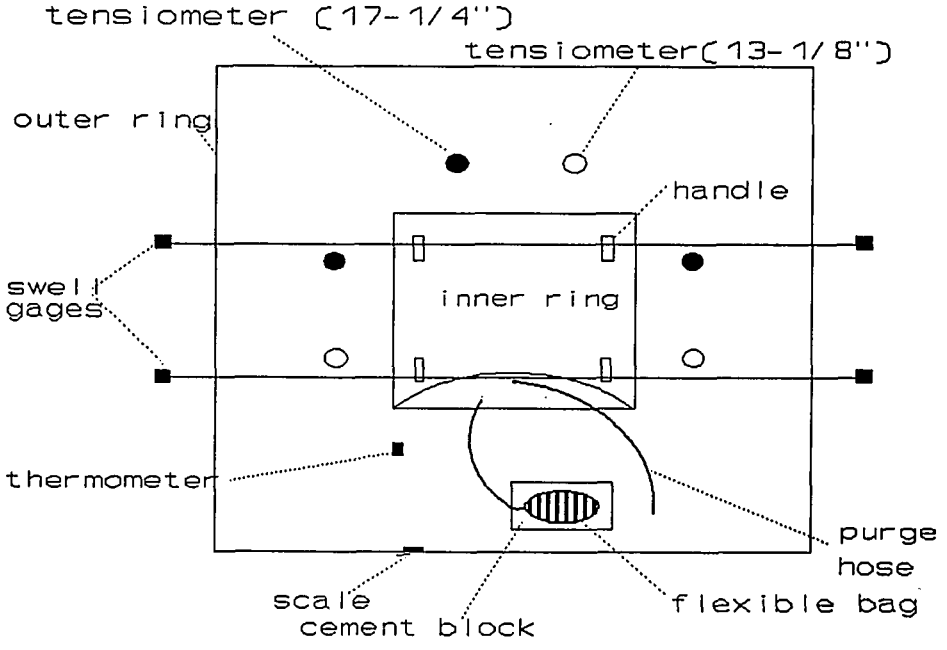


**Figure 3.1: SDRI Layout**

Initial Filling of the Rings

Two five gallon buckets of water were placed on the edge of the inner ring to prevent uplift as the inner ring was filled. The inner ring was partially filled with 15 gallons of water using a siphon. No leaks from the inner ring were apparent after waiting 30 minutes. The ports of the inner ring were left open so that it would finish filling as the outer ring was filled.

After giving the pad between the inner and outer rings a final cleaning, water was pumped from a nearby well to partially fill the outer ring to a level just above the ports of the inner ring. Cinder blocks were used to dissipate the force of the water from the hose in order to prevent scouring of the pad surface. No leaks from the outer ring were evident after waiting 1 hour. The outer ring was finally filled to its target depth of 12 inches, and the buckets holding down the inner ring were removed.

Initial Addition of Chemicals

Three chemicals were added to the water of the inner and outer rings at the time of filling: 1) calcium sulfate ($CaSO_4$), 2) potassium bromide (KBr), and 3) FD&C green #3 food coloring.

Calcium sulfate (0.01 N) was added to flocculate the clay, which promotes the highest permeability. The concentration of 0.01 N was suggested in by Daniel B. Stephens and Associates in a test manual for Weldon Springs, Missouri (DBS&A, 1991). Potassium bromide and the green food coloring were chosen as tracers that would identify the wetting front or preferential flow paths. The target concentrations were:

| | |
|---|---|
| $CaSO_4$ | 680 ppm |
| $Br^-$ | 60 ppm |
| green #3 | 80 ppm |

The target concentration for $CaSO_4$ was calculated as follows:

$$\left(\frac{0.01\ eqv}{1\ \ell}\right)\left(\frac{136.14\ g}{1\ mole}\right)\left(\frac{1\ mole}{2\ eqv}\right)\left(\frac{1000\ mg}{1\ g}\right)=680\ ppm \qquad (3.1)$$

Appropriate quantities of these chemicals were measured on a portable electric field scale and added to the initial 15 gallons of water before it was siphoned into the inner ring. The appropriate quantities of chemicals for a 6 inch increment of water depth in the outer ring were premixed in several five gallon buckets and then mixed into the outer ring as each 6 inches was filled. Quantity calculations are covered in a later section of this chapter.

Installation of Fittings

The inner ring slopes upward towards one end where three ports (two inlet and one outlet) were located. Brass and/or plastic fittings were used to close the ports or connect them to plastic hoses. The installation manual (Trautwein, 1991) contains diagrams of the fittings.

Prior to installation of fittings, which occurred under water, the inner ring was tapped with a broom handle until air bubbles stopped coming from the ports. All threaded parts were wrapped with teflon tape for better sealing, and all fittings and tubing were saturated with water and checked for air bubbles before installation.

One of the two inlet ports was closed with a plug fitting and fittings with barbed hose connectors were screwed into the remaining inlet port and the outlet port. A 3 foot piece of clear flexible tubing (3/8 inch diameter) was attached to the lower port (inlet port), and a 7 foot piece of the same tubing was attached to the upper port (outlet port). A brass plug was used to close the outlet or air purge hose. The inlet hose was rested on a cinder block under the water to await the attachment of the flexible bag. Figure 3.1 may be referred to for a schematic layout of the hoses.

Installation of the Outer Ring Cover

In order to reduce evaporation, maintain an even temperature, and prevent accumulation of debris in the outer ring, a 12 foot by 12 foot square cover was constructed of 2x4's and 3/4 inch plywood. It was insulated with R-16 foil-backed fiberglass insulation. Openings with removable covers allowed the inner ring and tensiometers to be serviced.

Installation of Swell Gages

Two swell gages were installed to measure any vertical movement of the inner ring. This arrangement consists of baling wire stretched between two metal fence posts driven into the pad several feet outside the outer ring. The fence posts for each swell gage were located so that the wire would pass directly over two of the handles on the inner ring. With two swell gages, therefore, the movement of all four handles could be monitored.

Using a caliper gage (accurate to 1 mm) attached to a metal rod, and the wires as reference elevations, the movement of each handle could be monitored. Bolts were attached to each handle to act as permanent reference points. The elevations of the wires and fence posts were referenced to a nearby temporary benchmark (a concrete well pad) to detect any movement of the wires themselves.

Attachment of the Flexible Bag

The flexible bag, which was really a plasma bag seen in hospitals everywhere, was filled by siphoning from a five gallon bucket of water (with chemicals) from the outer ring. It was alternatively filled and squeezed underwater in the bucket in order to remove all air bubbles. The final filling was slightly less than full so that the bag would not be under pressure when attached to the inner ring. A hose clamp was used to shut the short tube connector on the flexible bag.

After drying the flexible bag and hose clamp, it was weighed to the nearest 0.1 gram on a portable battery operated field scale. This initial weight was recorded. To be consistent with later weight measurements, the short length (approximately 1/2 inch) of the hose connector above the hose clamp was kept filled with water.

The flexible bag was lowered under the water in the outer ring and rested on a cinder block placed there for that purpose. After checking that neither the hose connector nor the 3 foot length of inlet hose contained air bubbles, the barbed tube connector was attached to the inlet hose.

## SDRI Operation and Data Collection

### Starting the SDRI Test

To start the test, the following data was recorded:

- date and time
- water temperature (°F)
- water level (inches)
- weight of flexible bag (grams)
- electrical conductivity of water in outer ring (umhos)
- tensiometer readings (centibars)
- swell gage readings (mm)

A swimming pool thermometer, which has a cup at the bottom to hold water when it is removed from the water, was hung by a string from the cover near the flexible bag. In addition, a water sample was collected from the outer ring to be later analyzed for bromide concentration. The hose clamp was opened and flow to the inner ring began, thus starting the infiltration measurements.

### Data Collection During the SDRI Test

Data was collected daily at first because of rapid initial infiltration, but by the end of the test, data was collected every 6 to 8 days. A total of 26 observations were made over 77 days. Data was collected at the same time of the day, about 8 AM, to eliminate diurnal variations as a source of error. Standardized forms were used to record the data.

The order of data collection was:

read swell gages (mm)
read tensiometers (centibars)
read water temperature (°F)
read water level in outer ring (inches)
remove and weigh flexible bag (g)
record date and time flexible bag removed
refill flexible bag
reweigh flexible bag (g)
purge air from inner ring if necessary
reattach flexible bag
record time flexible bag was reattached
refill outer ring
record new water level in outer ring (inches)

Swell Gage Measurements

With a caliper gage attached to an aluminum rod, the height of the swell gage wires was measured at each handle. A bolt had been attached to each handle to insure they were measured at the same place each time, and the caliper gage was left attached to the rod to prevent errors due to its movement. Measurements were to the nearest 0.1 mm.

Unfortunately, the rod and caliper gage were stolen in early May of 1991. They were not replaced and therefore swell measurements were taken only for the first two weeks of the test.

Tensiometer Readings and Maintenance

The tensiometers were simply read to the nearest centibar of suction. They were periodically maintained by adding fluid, deairing with a small suction pump, and tightening the caps. Even with such maintenance, only four of the six tensiometers functioned throughout the test.

Handling the Flexible Bag

Care was taken to eliminate sources of error in removing and weighing the flexible bag to reduce error. Prior to handling the flexible bag, the hose clamp was shut and the hose disconnected while under water. The open hose to the inner ring was rested on the cinder block to prevent mud or air from entering the hose. For consistent weight measurements, the hose connector and short length of hose above the hose clamp were always kept filled during handling. After drying the bag, it was weighed to the nearest gram with a portable electric scale.

Care was also taken to reduce error in filling and attaching the flexible bag. It was placed underwater in a five gallon bucket to be refilled by gravity siphoning. After connecting the flexible bag to a 3 foot length of hose and opening the hose clamp, the flexible bag was removed and lowered below the

level of the five gallon bucket, thus allowing gravity flow into the flexible bag without introducing air bubbles. The flexible bag was never filled completely so that it would not be under pressure. The flexible bag was replaced in the bucket to be disconnected underwater. After removing and drying the flexible bag, it was reweighed. Reattachment to the inner ring took place underwater and the hose clamp was not reopened until all air bubbles were removed from the hose.

The flexible bag was refilled only when half or more of its contents had flowed into the inner ring. When little flow occurred between observations, the flexible bag was simply removed, weighed, and reattached to the inner ring.

Monitoring and Adding Chemicals in the Inner Ring

The appropriate quantities of dye, potassium bromide, and calcium sulfate for 5 gallons of water were weighed in the laboratory (see later section in this chapter for quantities) and then added to the five gallon bucket of water used to refill the flexible bag. Thus chemicals were automatically added to the inner ring whenever the flexible bag was refilled. When not in use, the five gallon bucket was tightly sealed to prevent evaporation.

In order to monitor potassium bromide concentrations, water samples were occasionally collected from the five gallon bucket to later be analyzed for bromide with an ion specific probe. Calcium sulfate concentrations were monitored with a conductivity meter and previously established calibration curve. Conductivity readings were corrected for the background conductivity of the site water. Dye concentration was not monitored.

Purging Air from the Inner Ring

The 7 foot piece of clear hose attached to the outlet port was checked for air bubbles whenever the flexible bag was removed. No air bubbles were apparent until the latter part of the test. To remove air bubbles, the hose was unplugged and held underwater, thus allowing the bubbles to rise. The inner ring was tapped with a broom handle to loosen air bubbles, and the hose was purged as many times as needed. It was impossible to make accurate estimates of the amount of air purged because the process largely took place underwater.

Refilling the Outer Ring

The outer ring was refilled only when the water level had dropped 0.5 to 1.5 inches from the target depth of 12 inches.

Monitoring and Adding Chemicals in the Outer Ring

To maintain the potassium bromide and calcium sulfate, concentrations near their target levels, these chemicals were monitored both before and after refilling the outer ring. Water samples were collected before and after refilling to later be analyzed for bromide with a specific ion probe. Calcium sulfate was monitored in the field using a conductivity meter with a previously established calibration curve. Conductivity readings were corrected for the background conductivity of the site water. Dye concentration was not monitored because its concentration was not critical.

Chemical concentrations in the outer ring tended to increase with time because of evaporation, and therefore chemicals were not added every time the outer ring was refilled. Dye, potassium bromide, and calcium sulfate, which had been weighed and bagged in the laboratory for depth increments of 0.25, 0.5, and 1.0 inches in the outer ring, were premixed in a five gallon bucket and then added as the outer ring was refilled. Chemical quantities are covered in a later section of this chapter.

Bromide Measurement with a Specific Ion Probe

As mentioned previously, bromide concentrations in the outer ring and the five gallon bucket (for refilling the flexible bag) were sampled during operation for measurement in the laboratory. A Model 94-35 Bromide Electrode and Model 90-01 Double Junction Reference Probe (Orion Research Inc., Laboratory Products Group) were used with a direct calibration technique. A three point linear calibration curve of conductivity vs. concentration was established over a range of 0.8 to 79.9 mg/l. Concentrations were determined after each sampling in order to determine if chemicals should be added on the next visit to the site.

## Source Water for the SDRI

The initial source water for filling the SDRI was a nearby monitoring well (MW-2). A portable generator was available until the end of May for pumping the water. Table 3.1 compiles the results of a water quality analysis performed by a commercial laboratory in May, 1991. Electrical conductivity (EC) of the well water was 280 $\mu$mhos, as measured by the author with a field conductivity meter.

Table 3.1

**Water Quality Analysis for Selected Constituents in the Source Water (Monitoring Well #2)**

| Constituent | | Concentration (mg/l) |
|---|---|---|
| Chloride | Cl | 7.73 |
| Manganese | Mn | 0.402 |
| Sodium | Na | 33.0 |
| Sulfate | $SO_4$ | <5.0 |
| Bicarbonate | $HCO_3$ | 203 |
| Fluoride | F | 1.3 |
| Iodine | I | <0.5 |
| Phosphate, Total | $PO_4/T$ | <0.02 |
| Nitrate | $NO_3$ | 1.7 |

The portable generator was removed at the end of May, 1991 because of the rental expense. Two fifty-gallon drums, which were raised to allow siphoning, were located next to the SDRI to replace the well water. The drums were refilled on each data collection trip with five-gallon jugs of water from a convenience store in Catalina, Arizona, some 15 miles from the site. Water analyses were not performed on this water, but the electrical conductivity (EC) was 300 $\mu$mhos.

One concern with the source water, and particularly with changing the source water, was its effect on flocculating or dispersing the clay. The similar electrical conductivity

measurements indicated that the two source waters would affect the clay similarly. Moreover, the addition of $CaSO_4$ at a target concentration of 680 ppm was intended to flocculate the clay and raised the electrical conductivity to about 1000 $\mu$mhos, which more or less swamps the effect of the background conductivity.

## Chemical Quantities for Initial Filling and Operation

Table 3.2 summarizes the chemical quantities used for the initial filling of the inner and outer rings, as well as the quantities used for refilling the inner and outer rings during operation. The quantities for a five gallon bucket were used for the inner ring, both the initial filling and refilling during operation. The 6 inch quantity was used for the initial filling of the outer ring and the 0.25, 0.5, and 1.0 inch quantities were used for refilling the outer ring during operation.

**Table 3.2**

**Chemical Quantities for Initial Filling and Operation**

| Chemical | Target (mg/l) | Quantity (g) for 5-gal. Bucket or Depth of Water in Outer Ring: 5-gal. Bucket | 0.25" | 0.5" | 1" | 6" |
|---|---|---|---|---|---|---|
| $CaSO_4$ | 680 | 12.9 | 54.8 | 109.5 | 219 | 1314 |
| KBr | 60 | 1.7 | 7.2 | 14.3 | 28.7 | 172 |
| Dye | 80 | 1.5 | 6.4 | 12.8 | 25.7 | 154 |

Sample Calculation for 1" Depth in Outer Ring:

$$Vol. = (19600\ inch^2)(1''\ deep)\left(\frac{16.39\ cm^3}{inch^3}\right)\left(\frac{1\ \ell}{1000\ cm^3}\right) = 321.2\ l$$

$$\left(\frac{680\ mg\ CaSO_4}{1\ \ell}\right)(321.2\ \ell)\left(\frac{1\ g}{1000\ mg}\right) = 219\ g\ CaSO_4$$

$$\left(\frac{60\ mg\ Br^-}{1\ \ell}\right)(321.2\ \ell)\left(\frac{1\ g}{1000\ mg}\right)\left(\frac{119\ g\ KBr}{80\ g\ Br^-}\right) = 28.7\ g\ KBr$$

$$\left(\frac{80\ mg\ dye}{1\ \ell}\right)(321.2\ \ell)\left(\frac{1\ g}{1000\ mg}\right) = 25.7\ g\ dye$$

## SDRI Removal and Data Collection

### Dismantling the SDRI

After removing the swell gages and flexible bag, the wood cover was dismantled so that the plywood could later be reused. The outer ring was drained with five gallon buckets to within several inches of the pad and a corner of the outer ring was lifted loose, thus allowing the outer ring to completely drain. After removing the tensiometers, the soft clay was covered with plywood to provide a working area between the inner and outer rings. The inner ring was pulled out, the water drained, and the surface was covered with two layers of black plastic until sampling could begin on the next day.

### Data Collection During SDRI Removal

Time domain reflectometry (TDR) was used to measure in-situ volumetric water content with depth in a trench through the inner ring. Four profiles were measured from the surface to about 20 cm deep at 1 to 5 cm intervals. The instrument was a Tektronix 1502B with a probe length and spacing of 15 cm and 2.5 cm, respectively. The length of trace was calibrated for the dielectric constant of water in a bucket of water using a multiplier of 0.33.

A grid of 16 points was set up on the 5 foot by 5 foot inner ring in order to collect clay samples. Sampling points were located at 1 foot intervals with all outer points set 1 foot in from the edge of the inner ring to avoid edge effects. The pad was trenched along the grid lines and samples cut out with a trowel. The sample size was approximately 8 cubic inches. Samples were taken at 2 cm intervals down to a depth of 10 cm at each grid point, except at four grid points (1A, 1B, 1C, and 1D) where they were taken to a depth of 20 cm. A total of 100 samples were collected.

The wet clay samples were labelled and double-bagged in plastic bags. Back at the laboratory, they were air dried for a week to await extraction of the soil solution for bromide testing.

Core samples were taken at the four corners of the pad between the inner and outer rings; these will be further discussed under the section Geotechnical Testing.

Figure 3.2, Data Collection During SDRI Removal, shows the location of all sampling points for the TDR, clay samples, and core samples.

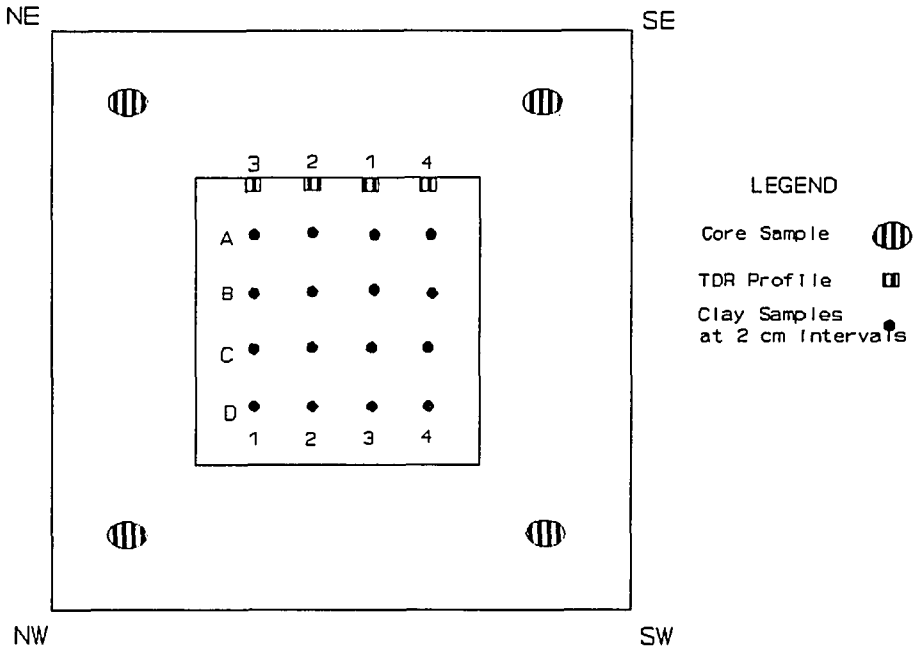


**Figure 3.2: Data Collection During SDRI Removal**

## Geotechnical Testing

### Bulk Density and Gravimetric Water Content

Undisturbed core samples for bulk density were taken from the southwest corner of the pad (outside the outer ring of the SDRI) on May 13, 1991. A thin walled sampler (2 inch diameter) was used to collect samples at four depths from 0 to 18.25 inches. Samples were weighed, dried at 105 °C for 24 hours, and reweighed to determine bulk density and gravimetric water content.

Four more undisturbed core samples were taken during SDRI removal on July 10, 1991 by Desert Earth Engineering. Three samples at 0.5 foot increments were taken at each corner of the pad between the rings, for a total of twelve samples; each core was 6 inches long by 3 inches in diameter. The author dried half of the samples (i.e., the samples from the southeast and southwest corners) at 111 °C until their weight no longer decreased in order to calculate bulk density and gravimetric water content.

One of the undisturbed cores mentioned in the previous paragraph was sent to Daniel B. Stephens and Associates, Inc. for testing. Bulk density, initial water content, and porosity were calculated after weighing the wet sample, drying

for 24 hours at 105 °C, and reweighing. Other tests performed by these consultants are discussed in later sections.

Atterberg Limits

The Atterberg limits were determined on a sample of uncompacted clay by Desert Earth Engineering on March 26, 1991 as part of the clay selection process. In November, 1991, Desert Earth determined the Atterberg limits on 4 remolded samples from the test pad. In both cases the ASTM D 4318 (1990) procedure was used.

GRC Consultants also determined the Atterberg limits with uncompacted clay collected on April 23, 1991 during construction of the pad; the test procedure was not specified.

Grain Size Distribution

Desert Earth Engineering determined the grain size distribution twice during the project using ASTM D 422 (1990) for particles larger than a No. 200 sieve and ASTM D 1140 (1990) (hydrometer test) for particles smaller than a No. 200 sieve. Grain size distribution was determined on one uncompacted clay sample in March, 1991, and on four core samples taken from the test pad in November, 1991. GRC Consultants, Inc. determined the grain size distribution of

one sample of uncompacted clay taken during construction in April, 1991; no test procedure was specified.

Proctor Tests

Desert Earth Engineering performed one standard Proctor test (ASTM D 698, 1990) on a sample of uncompacted clay as part of the clay selection in March, 1991. In November, 1991, they conducted standard Proctor tests on four remolded core samples taken from the test pad; ASTM D 698 (1990) was again used.

Permeability Tests

Desert Earth Engineering conducted a flexible wall conductivity test (EPA Method 9100-19) on a sample of clay remolded to 95% of standard Proctor density (ASTM D 698, 1990) at a moisture content 3% above optimum. This test was conducted in March, 1991 as part of the clay selection process.

Western Technologies, Inc. conducted a flexible wall permeability test on two undisturbed core samples from the test pad. The samples were taken from 0.0 to 0.5 feet and 0.5 to 1.0 feet in depth on October, 29, 1991. A test procedure was not specified, but the test was performed with a 5 psi differential pressure and a confining pressure of 2 psi.

In August of 1991 Daniel B. Stephens and Associates, Inc. conducted a falling head permeability test on an undisturbed core taken on July 10, 1991 from the northeast corner of the test pad at a depth of 0.0 to 0.5 feet. Two tests of 24 hours each were performed to estimate an average saturated hydraulic conductivity. The sample length was 3.6 cm and its cross sectional area was 29.13 $cm^2$.

Soil Moisture Release Curves

In August of 1991 Daniel B. Stephens and Associates, Inc. established a soil moisture release curve for an undisturbed core sample taken on July 10, 1991 at a depth of 0.0 to 0.5 feet from the northeast corner of the test pad. The sample volume was 107.74 $cm^3$, its dry weight was 205.77 g, and its saturated moisture content was 30.04 %. A 15 bar pressure plate was used and the suction head was varied from 0.0 to 14.7 bars in four steps for a total of five data points. The test took about two weeks.

Soil Identification

The clay was described as a red clay by Desert Earth Engineering in March, 1991, and was classified as a sandy, fat clay with gravel (CH) using ASTM D 2488 (1990). In May, 1991, GRC Consultants, Inc. described the same clay as a reddish

brown clayey sand (SC) according to the Unified Soil Classification System (USCS) system.

## Laboratory Analysis for Bromide Tracer

### Clay Solution Extraction

The method of Chapter 10, Soluble Salts, from Methods of Soil Analysis (Soil Science Society of America, Inc., 1982) was adapted for the clay samples collected during SDRI removal. Solution extraction with a suction filter apparatus was impossible because of the low permeability of the compacted clay.

The air-dried samples were first broken up with a hammer to a uniform mixture, and then weighed to the nearest gram. After placing the sample in a 1000 ml Erlenmeyer flask, a volume of deionized water equal to the weight of the sample was added to the flask (i.e., a 1:1 soil/water ratio). The flask was stoppered and shaken vigorously by hand for 1 minute for four times at 30 minute intervals.

The mixture was allowed to settle until the supernatant was clear, usually 24 to 48 hours. The supernatant was pipetted off and filtered through a 0.45 micron filter to remove any remaining particulates. From 25 to 100 ml of solution were extracted, depending on the size of the clay sample.

Extracted solution samples were labelled and stored in plastic bottles until the bromide concentrations were measured.

Bromide Measurement with a Specific Ion Probe

As a first attempt at measuring bromide concentrations in the extractions, a Model 94-35 Bromide Electrode and Model 90-01 Double Junction Reference Probe (Orion Research Inc., Laboratory Products Group) were used with a direct calibration technique. A three point linear calibration curve was established over a range of 0.8 to 79.9 mg/l. Unfortunately, most of the resulting bromide measurements were scattered around the background values, and thus were useless. The ion chromatograph was chosen as a better measurement method.

Bromide Measurement with an Ion Chromatograph

Bromide concentrations were measured with an ion chromatograph with the following equipment: Spectra Physics Model 8700 Delivery System, Spectra Physics Model 8750 Organizer/Pump, Dionex Model ASA4 P/N 37014 Column, Dionex Model AMMS-I P/N 038019 Micromembrane Suppressor, Dionex Model CDM-2 Conductivity Detector, Spectra Physics Model 4100 Computing Integrator. Two eluants were used (50% 3.7 mM $NaHCO_3$ and 50% 3.6 mM $Na_2CO_3$) and 0.25 N $H_2SO_4$ was used as the regenerent for

the suppressor column. Flow rate was maintained constant at 3 to 5 ml/minute.

A five point linear calibration curve of peak height with bromide concentration was established at the start of each day and at least one point on the curve was rechecked every 15 to 20 samples. The linear range was 0.2 mg/l to 8 mg/l. Because the bromide concentrations of the extractions from 2 cm depth were expected to be outside this linear range, these extractions were diluted by 1 ml in 9 ml of deionized water. The bromide concentrations at all other depths fell within the linear range and needed no dilution.

Although bromide concentrations in the outer and inner rings were monitored with a specific ion probe during the test, four samples were remeasured with the ion chromatograph in order to provide a consistent set of data. These samples were also diluted by 1 ml in 9 ml to fall within the linear range of the calibration curve for the ion chromatograph.

# CHAPTER 4

# DATA REDUCTION

Much of the data collected during the SDRI test required manipulation before it could be analyzed. This chapter describes the equations used and calculations performed, as well as discussions of data error where appropriate; if the raw data did not require manipulation, then it is included in Chapter 5 as results.

## Reduction of Tensiometer Data

Only four of the six tensiometers survived the three-month SDRI test in working order. One of these was at a depth of 13-1/8 inches and the other three were at a depth of 17-1/8 inches. The length of the ceramic cup was 2 inches, thus placing the center of the ceramic cup at 12-1/8 inches and 16-1/8 inches for the two tensiometer depths, respectively. The pressure gauges were 12 inches above the surface of the pad for all tensiometers.

To calculate head in cm from the recorded tension in centibars, the centibar readings were first converted to pressure in pascals, which are equivalent to $N/m^2$, by multiplying by 1000 Pa/centibar. Head in cm was then calculated with the following equation:

$$h = \left( \frac{-p_{gauge}}{\rho g} \right) 100 + \Delta Z_1 + \Delta Z_2 \qquad (4.1)$$

where:
- h = negative pressure or suction head (cm)
- $\Delta Z_1$ = height of gauge above pad (cm)
- $\Delta Z_2$ = depth of center of cup below pad (cm)
- $\rho g$ = 9810 $N/m^3$
- $p_{gauge}$ = centibar reading converted to $N/m^2$
- 100 = 100 cm/m

Table A1 in the Appendix contains the tensiometer calculations. Note that the maximum suction recorded by any of the tensiometers was 0.48 bar (48 cb), which was well within the useful limit of about 0.8 bar (80 cb) of most tensiometers (Hillel, 1982).

## Reduction of TDR Data

As described in Chapter 3, Procedures, TDR was used to obtain four water content profiles during removal of the SDRI. The length of trace ($L_{trace}$), which is recorded in the field, must be converted to the dielectric constant (K) in order to be used in an empirical regression equation between K and water content (Topp et al., 1980). To convert $L_{trace}$ to K, the following equation was used:

$$K=\left(\frac{L_{trace}*multiplier}{L_{probe}}\right)^2 \qquad (4.2)$$

where: K = dielectric constant
$L_{trace}$ = length of trace (cm)
$L_{probe}$ = length of probe (15 cm)
multiplier = 0.33

Topp's regression equation to obtain water content from K is given below:

$$\theta_v=-5.3*10^{-2}+2.92*10^{-2}K-5.5*10^{-4}K^2+4.3*10^{-6}K^3 \qquad (4.3)$$

where: $\theta_v$ = volumetric water content
K = dielectric constant

Table A4 in the Appendix shows the TDR data and water content calculations and Figure 4.1 depicts the data graphically.

Although the water content data in Figure 4.1 exhibit scatter, they show a general trend of a wet area near the pad surface, a slightly drier area between 3 and 7 cm, and then increasing wetness with depth. The four profiles, which were taken along one five foot long transect (see Figure 3.2, Chapter 3, Procedures), were insufficient to say anything about the heterogeneity of the 25 square foot inner ring. Moreover, some of the scatter was due to operator error, such as difficulties in pushing the probe straight into the hard clay, and data reduction error due to the applicability of the Topp equation. Although Topp et al. (1980) based the regression on a variety of soils, its accuracy in compacted clay was not known.

In short, error in the TDR water content data could not be assessed and the scatter was probably due to data collection/reduction error and heterogeneity of the material. However, when converted to gravimetric water content, the range of TDR water contents from 0.12 to 0.15 compared favorably to the gravimetric water contents of 0.09 to 0.16 from pre- and post-construction core samples.

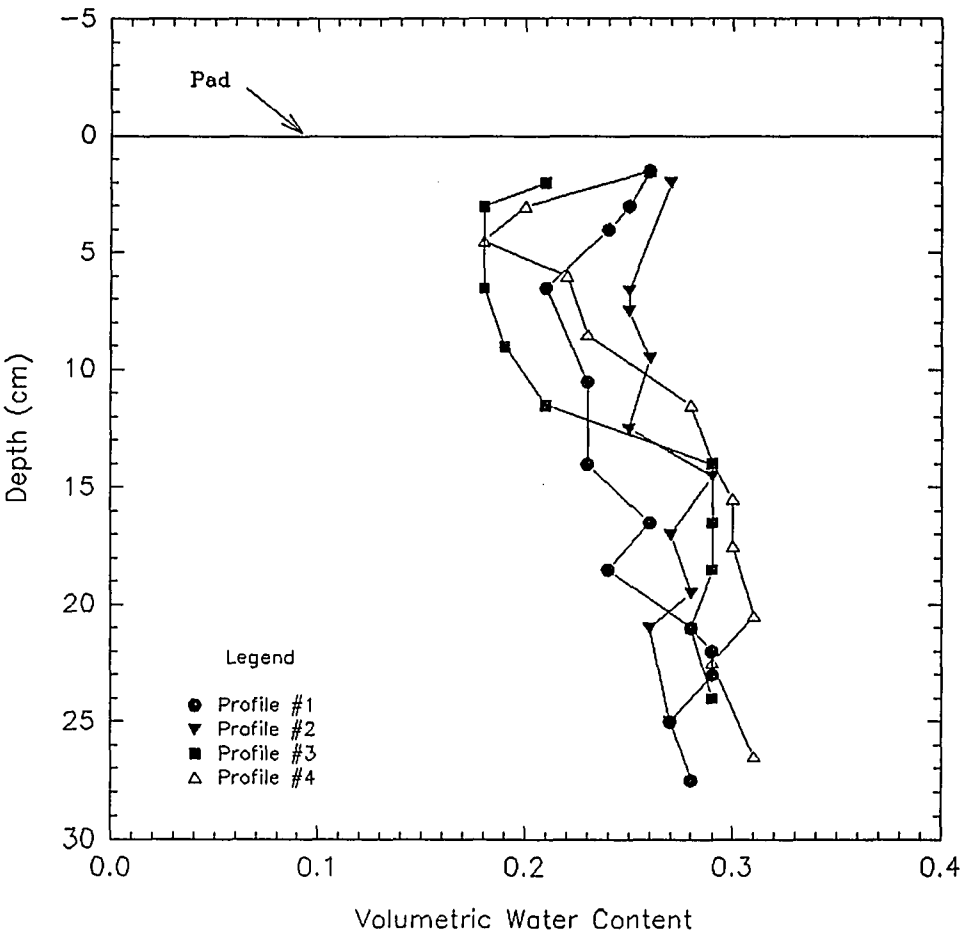


**Figure 4.1: TDR Volumetric Water Content**

## Infiltration Calculations

The infiltration rate (I) was calculated according to the equations in the Installation and Operating Instructions for the Sealed-Double Ring Infiltrometer (Trautwein, 1991).

$$I = \frac{Q}{At} \qquad (4.4)$$

where: I = infiltration rate (cm/sec)
Q = volume of flow from the flexible bag ($cm^3$) corrected for temperature-dependent density changes
A = area of flow in the inner ring ($cm^2$)
t = time interval in which Q was measured (sec)

The measured flow was simply the weight of the flexible bag when it was removed subtracted from the weight when it was attached. The density of water, $\rho$ ($g/cm^3$), was used to convert the flow measurements by weight (g) to flow measurements by volume ($cm^3$). However, the density of water is temperature dependent, and an equation developed by Daniel B. Stephens and Associates, Inc. (DBS&A) (1991) was used to correct density for temperature. DBS&A in turn based their regression equation on data presented by Vennard and Street (1982):

$$\rho = 0.9998 + 7.1162 * 10^{-5} T - 9.2484 * 10^{-6} T^2 + 7.5070 * 10^{-7} T^3 \qquad (4.5)$$

where: T = average temperature (°C) for time interval in which Q was measured
$\rho$ = density ($g/cm^3$)

To summarize, the temperature corrected flow by volume, Q, was calculated as follows:

$$Q = \frac{weight\ on - weight\ off}{\rho} \qquad (4.6)$$

where:
Q = volume of flow ($cm^3$)
weight on = weight of the flexible bag when attached (g)
weight off = weight of the flexible bag when removed (g)

Trautwein (1991) suggests that the flow rate, Q, also be corrected for swelling of the clay. Unfortunately, the swell gage was stolen at Page Ranch before enough data could be collected to tell if swell had occurred.

The time interval in which the flow rate was measured was simply the time on and time off corresponding to attaching and removing the flexible bag. The time interval was converted to seconds for use in Equation 4.5. Table A3 in the Appendix summarizes the raw data and infiltration rate calculations.

## Hydraulic Gradient Calculations

The hydraulic gradient, i, was simply the head loss (Δh) divided by the length of flow path over which the head loss occurred (Δs). As shown in Equation 4.6, head loss was comprised of the depth of water in the outer ring, the depth of the wetting front, and the suction head at the wetting front; the length of flow path was simply the depth of the wetting front.

$$i = \frac{\Delta h}{\Delta s} = \frac{H + D + H_s}{D} \qquad (4.7)$$

where:
- i = gradient (dimensionless)
- Δh = head loss (cm)
- Δs = flow path over which Δh occurred (cm)
- H = time-averaged depth of water in the outer ring (cm)
- D = depth of the wetting front (cm)
- $H_s$ = suction head at the wetting front (cm)

Because the depth, or head, in the outer ring varied with evaporation and refilling, the time-averaged head was calculated. Depth was recorded as "depth off" when the flexible bag was removed, and as "depth on" when the flexible bag was reconnected. The average depth for the time period between readings was simply the sum of the on and off readings divided by two. The total time of the test was 75.28 days,

and the average heads for each time period, which varied from 1 to 8 days, were time-averaged as follows:

$$h = \frac{\Sigma(av.\ depth * time\ interval)}{total\ time} \qquad (4.8)$$

where:
- h = time averaged depth (cm)
- av. depth = average depth in a time interval (cm)
- time interval = time between attaching and removing the flexible bag (days)
- total time = total time of SDRI test (days)

Table A2 in the Appendix contains the calculations for the time-averaged head in the outer ring.

Neither visual means nor physical measurements could pinpoint the wetting front because of shortcomings in the instrumentation and the diffuse nature of a wetting front in compacted clay. Estimating the suction head at the wetting front is not straight forward either, and a thorough discussion of this parameter, as well as the depth of the wetting front, is contained in Chapter 5, Results and Analysis.

## Calculation of Bromide Concentrations

The bromide concentrations measured by the ion chromatograph could not be interpreted until field concentrations were back calculated with the appropriate dilution factors. Calculations are shown in Table A5 in the Appendix. Two types of dilution were used during analysis:

1) Extraction dilution factor. At the time of sampling, the clay samples contained some pore water, with those from behind the wetting front containing higher water contents than those from in front of the wetting front. Air drying of the samples, of course, removed that water. The 1:1 extraction process added a volume of water equal to the air dry weight of the sample, thus diluting the bromide that was originally in solution in the pore water. This dilution factor (D.F.) was calculated as follows:

$$D.F. = \frac{vol.\ water\ added - vol.\ water\ original}{vol.\ water\ original} \qquad (4.9)$$

where: volume water added (ml) = weight of air dry sample (g)

volume water original (ml) = weight water original (ml) = $(\theta)$(weight of air dry sample (g)

$\theta$ = gravimetric water content (g/g)

$\rho_w$ = density of water = 1.0 g/cm$^3$

2) Ion chromatograph dilution factor. Because the expected concentrations of the extractions at a depth of 2 cm and the water samples from the inner and outer rings were well outside of the linear range of the calibration curve, these samples were diluted with 1 ml of sample in 9 ml of deionized water. The resulting dilution factor is 10. All other samples did not need to be diluted and therefore received a dilution factor of 1 in the spreadsheet calculations.

Two sources of error contributed to uncertainty in the back calculated field bromide concentrations. First, variation in the ion chromatograph readings constitutes a source of error that could be quantified by precision and accuracy. Second, uncertainty in estimating the water content at the time the SDRI was drained lead to variation in the dilution factor.

In the course of ion chromatograph work six samples were repeated, and although these two replicates did not allow detailed statistical analysis, some inferences regarding precision could be made. As shown in Table 4.1, the mean difference between the replicates was 0.1 mg/l $Br^-$ with a standard deviation of 0.1 mg/l. Overall, the data set was

quite precise before back calculation of field values with extraction dilution factors.

**Table 4.1**

**Ion Chromatograph Precision Analysis**

| Sample | Replicate #1 $Br^-$ (mg/l) | Replicate #2 $Br^-$ (mg/l) | Difference (mg/l) \| #2 - #1 \| |
|---|---|---|---|
| 4A-4 | 4.9 | 4.9 | 0.0 |
| 1C-4 | 6.2 | 5.9 | 0.3 |
| 3C-4 | 5.9 | 5.9 | 0.0 |
| 4C-4 | 6.4 | 6.3 | 0.1 |
| 2D-4 | 6.9 | 7.0 | 0.1 |
| 3D-4 | 5.6 | 5.7 | 0.1 |
| | | Mean | 0.1 |
| | | Standard Deviation | 0.1 |

Accuracy of the measurements was determined from repeated measurements of bromide standards as shown in Table 4.2. Except for the 4.0 mg/l standard, the mean of all measurements for each standard fell within one standard deviation of the standard. The mean of 3.8 mg/l with a standard deviation of 0.1 mg/l was slightly lower than the standard of 0.4 mg/l. Overall, the ion chromatograph accuracy could be characterized as ±0.1 mg/l, assuming, of course, that the lab standards were the "true" concentration.

**Table 4.2**

**Ion Chromatograph Accuracy Analysis**

| | Standard (mg/l) | | | | |
|---|---|---|---|---|---|
| Measurement | 8.0 | 4.0 | 0.8 | 0.4 | 0.2 |
| 1 | 8.0 | 3.8 | 0.8 | 0.4 | 0.3 |
| 2 | 8.0 | 3.8 | 0.8 | 0.4 | 0.2 |
| 3 | 8.0 | 3.7 | 0.8 | 0.5 | 0.3 |
| 4 | 8.1 | 3.9 | 0.9 | 0.4 | 0.3 |
| 5 | 8.1 | 3.6 | 0.9 | 0.5 | 0.2 |
| 6 | 8.1 | | 0.9 | | 0.3 |
| 7 | 8.2 | | 0.8 | | |
| 8 | 8.1 | | 0.9 | | |
| 9 | 8.2 | | 0.8 | | |
| 10 | | | 0.9 | | |
| 11 | | | 0.9 | | |
| n | 9 | 5 | 11 | 5 | 6 |
| Mean (mg/l) | 8.1 | 3.8 | 0.9 | 0.4 | 0.3 |
| Std. Dev. (mg/l) | 0.1 | 0.1 | 0.1 | 0.1 | 0.1 |

Due to uncertainty in estimating the gravimetric water content at the time of sampling, the other major source of error was the dilution factor for the extractions. In other words, the back calculated bromide concentrations, or field concentrations, were only as good as the estimate of the volume of pore water that originally contained the bromide in solution. Given that the error in the TDR water content data could not be assessed and that an overall trend was apparent

in the TDR data (see previous section on Reduction of TDR Data), the practical question was whether to vary water content with depth or to use a constant water content with depth.

Field bromide concentrations would be affected in two ways: 1) the ±0.1 mg/l error from the ion chromatograph would be multiplied by either a variable or constant dilution factor, and 2) the ion chromatograph bromide concentration would be multiplied by either a variable or constant dilution factor, resulting in a range of field bromide concentrations that cannot be strictly considered "error". Because it was difficult to explore these effects without looking at example data, bromide profile 1A was arbitrarily selected for study as representative of all the profiles.

If gravimetric water content was varied from 0.12 to 0.15, as suggested by the overall trend shown in Figure 4.1, the resulting dilution factors for bromide profile 1A would vary from 5.8 to 7.6. On the other hand, the average gravimetric water content was 0.13, which corresponded to an average dilution factor of 6.7. These values were visually estimated from Figure 4.1 as the midpoint of the band of volumetric water contents at a given depth; a bulk density of 1.89 g/cm$^3$

was used to convert volumetric water content to gravimetric water content. Table A7 in the Appendix compiles these calculations.

The effect of multiplying the ±0.1 mg/l ion chromatograph error by the dilution factor can be explored analytically. If the constant dilution factor of 6.7 was multiplied by ±0.1 mg/l, the resulting error would be ±0.67 mg/l. If a variable dilution factor of 5.8 to 7.6 multiplied the ±0.1 mg/l error, the resulting error would vary from 0.58 to 0.76 mg/l. Table A8 in the Appendix provides an example of this effect on bromide profile 1A. The difference between the two approaches, constant or variable dilution factor, was not great, and the resulting error in field bromide concentrations due solely to ion chromatograph error can be generalized as ±0.7 mg/l.

Multiplying the ion chromatograph concentrations by a constant or variable dilution factor produced a range of field concentrations that overshadowed the effect of multiplying the ±0.1 mg/l ion chromatograph error. Table 4.3 summarizes the calculations of Table A8 in the Appendix for bromide profile 1A and shows that the difference in field concentrations (without considering the ±0.1 mg/l ion chromatograph error)

was as much as 7.2 mg/l and as little as 0.4 mg/l. The average difference was 2.5 mg/l.

**Table 4.3**

**Difference in Bromide Concentrations Due to Constant or Variable Dilution Factors for Profile 1A**

| Sample | Field $Br^-$ Concentrations | | Difference (mg/l) |
|---|---|---|---|
| | Constant D.F. (mg/l) | Variable D.F. (mg/l) | |
| 1A-2 | 120.0 | 127.2 | 7.2 |
| 1A-4 | 48.5 | 52.8 | 4.3 |
| 1A-6 | 41.6 | 47.2 | 5.6 |
| 1A-8 | 23.4 | 25.2 | 1.8 |
| 1A-10 | 24.0 | 25.1 | 1.1 |
| 1A-12 | 22.6 | 22.2 | 0.4 |
| 1A-14 | 16.7 | 15.7 | 1.0 |
| 1A-16 | 14.4 | 12.9 | 1.5 |
| 1A-18 | 10.6 | 9.3 | 1.3 |
| 1A-20 | 7.8 | 6.8 | 1.0 |

In addition to viewing the two aforementioned effects separately, they can be combined to obtain a range of field bromide concentrations that reflects the ±0.1 mg/l ion chromatograph error and the constant or variable dilution factor. Table 4.4, which again summarizes the calculations of Table A8 in the Appendix, shows that the range of field bromide concentrations was as great as 7.7 mg/l and as little

as 0.5 mg/l. The average range was 2.7 mg/l. The range was defined as the difference between the two values produced by +0.1 mg/l error and constant dilution factor and +0.1 mg/l error and variable dilution factor, or the two values produced by -0.1 mg/l error and constant dilution factor and -0.1 mg/l error and variable dilution factor, whichever was greatest. Values with +0.1 mg/l error were not compared to values with -0.1 mg/l error because the ion chromatograph error cannot be plus and minus for the same measurement.

**Table 4.4**

**Combined Effect of Ion Chromatograph Error and Constant or Variable Dilution Factor for Profile 1A**

| | Field $Br^-$ Concentrations | | | | |
|---|---|---|---|---|---|
| | Constant D.F. | | Variable D.F. | | |
| Sample | +0.1 mg/l | -0.1 mg/l | +0.1 mg/l | -0.1 mg/l | Range (mg/l) |
| 1A-2 | 126.7 | 113.3 | 134.4 | 120.1 | 7.7 |
| 1A-4 | 49.2 | 47.8 | 53.5 | 52.1 | 4.3 |
| 1A-6 | 42.1 | 40.9 | 48.0 | 46.4 | 5.8 |
| 1A-8 | 24.1 | 22.8 | 25.9 | 24.5 | 1.8 |
| 1A-10 | 24.7 | 23.3 | 25.9 | 24.5 | 1.2 |
| 1A-12 | 23.3 | 21.9 | 22.8 | 21.5 | 0.5 |
| 1A-14 | 17.4 | 16.0 | 16.2 | 15.0 | 1.2 |
| 1A-16 | 15.1 | 13.7 | 13.5 | 12.3 | 1.6 |
| 1A-18 | 11.2 | 9.9 | 9.8 | 8.7 | 1.4 |
| 1A-20 | 8.5 | 7.2 | 7.3 | 6.2 | 1.2 |
| | | | Average Range | | 2.7 |

Based on these values, the difference between using a constant or variable dilution factor seemed unimportant and the computationally simpler method of an average dilution factor was adopted. Assuming that this one bromide profile was representative of all the profiles, the average range of possible values in the field bromide concentrations can be as generalized as 2.7 mg/l, which corresponds to ±1.4 mg/l.

# CHAPTER 5

# RESULTS AND ANALYSIS

## Engineering Description of the Compacted Clay

Because the test pad is not a natural material, such as soil or an aquifer, this section provides an engineering description of the compacted clay. This information is provided as background and is not used in later hydrologic calculations.

Particle size analysis showed that, on the average, the compacted clay is 60% sand and gravel and that silt and clay are 20% each. The construction specification for the test pad called for all particles to be smaller than 2 inches, but did not specify a median diameter ($D_{50}$) or a minimum clay content. Table 5.1 shows the results of the particle size analysis performed by several subconsultants on the project. Size classes are based on the ASTM classification system.

Table 5.2 compiles information on dry bulk density($\rho_d$), water content (gravimetric, $\theta$, and volumetric, $\theta_v$), and porosity ($\eta$). In addition to this geotechnical data, field tests during construction showed relative compaction greater than 100% of maximum standard Proctor density. The data are

Table 5.1

Particle Size Distribution of the Compacted Clay

| Sample (Date) | % gravel | % sand | % silt | % clay | $D_{50}$ mm |
|---|---|---|---|---|---|
| GRC (April, 1991) | 14 | 41 | 13 | 41 | 0.146 |
| DEE (March, 1991) | 33 | 13 | 13 | 41 | 0.032 |
| DEE (Nov., 1991) | | | | | |
| Composite | 17 | 46 | 19 | 18 | 0.038 |
| NE corner | 27 | 38 | 27 | 8 | 0.047 |
| NW corner | 24 | 47 | 24 | 5 | 0.052 |
| SW corner | 16 | 49 | 27 | 8 | 0.034 |
| Average | 21 | 39 | 20 | 20 | 0.052 |

GRC=GRC Consultants, Inc.
DEE=Desert Earth Engineering

gravel: 75-4.75 mm  sand: 4.75-0.075 mm
silt: 0.075-0.005 mm  clay: 0.005-0.001 mm

based on core samples taken at various times throughout the SDRI test, and some values are averages for subsamples of the same core taken at different depths. No trends with depth were apparent from the core samples. Note that porosity is calculated assuming a particle density of 2.65 g/cm$^3$.

Table 5.2

**Dry Bulk Density, Water Content, and Porosity from Undisturbed Core Samples**

| Sample (Date) | $\rho_d$ g/cm$^3$ | $\theta$ % | $\theta_v$ % | $\eta$ % |
|---|---|---|---|---|
| UA, swc(May, 1991) | 1.93 | 12 | 23 | 27 |
| UA, sec(July, 1991) | 1.90 | 14 | 26 | 30 |
| UA, swc(July, 1991) | 1.80 | 14 | 26 | 31 |
| DBS&A, nec(July, 1991) | 1.91 | 15 | 29 | 29 |
| Average | 1.89 | 14 | 26 | 29 |

UA=University of Arizona
DBS&A=Daniel B. Stephens & Assoc., Inc.

swc: southwest corner of test pad
sec: southeast corner of test pad
nec: northeast corner of test pad

Desert Earth Engineering determined the Atterberg limits on 5 different samples throughout the project. The average liquid limit (LL) and plasticity index (PI) were 44 and 26, respectively, but the LL and PI were as high as 68 and 42,respectively. A plot of these values on Casagrande's plasticity chart (Holtz and Kovacs, 1981) indicated that the clay faction was composed solely of montmorillonite and illite.

The March, 1991 sample was identified by Desert Earth Engineering under the ASTM classification system as a sandy, fat clay with gravel (CH); the April, 1991 sample was identified by GRC, Inc. under the USCS classification system as a reddish brown clayey sand (SC). Note that a material must have at least 50% silt and clay to be classified as fine-grained under either system, and that the "red clay" used at Page Ranch could not always be classified as a clay.

### Water Temperature in the Outer Ring

Because the SDRI test began in April and ran until early July, the water in the outer ring was subjected to the hot, dry weather typical of the Sonoran Desert in May and June. As shown in Figure 5.1, water temperature rose at a more or less constant rate throughout the test. Data always was collected between 7 AM and 9 AM and therefore the rise depicted in Figure 5.1 does not reflect diurnal fluctuations.

Because flow measurements from the flexible bag depended on using density to convert the weight of water to a volume of water, and because density is inversely proportional to temperature, the water temperature becomes an important variable. As discussed in Chapter 4, Data Reduction, flow

rates were corrected for temperature-dependent density changes. If Trautwein's (1991) recommendation to disconnect the flexible bag when temperature changed by more than 1 °C had been followed, the test could never have been completed.

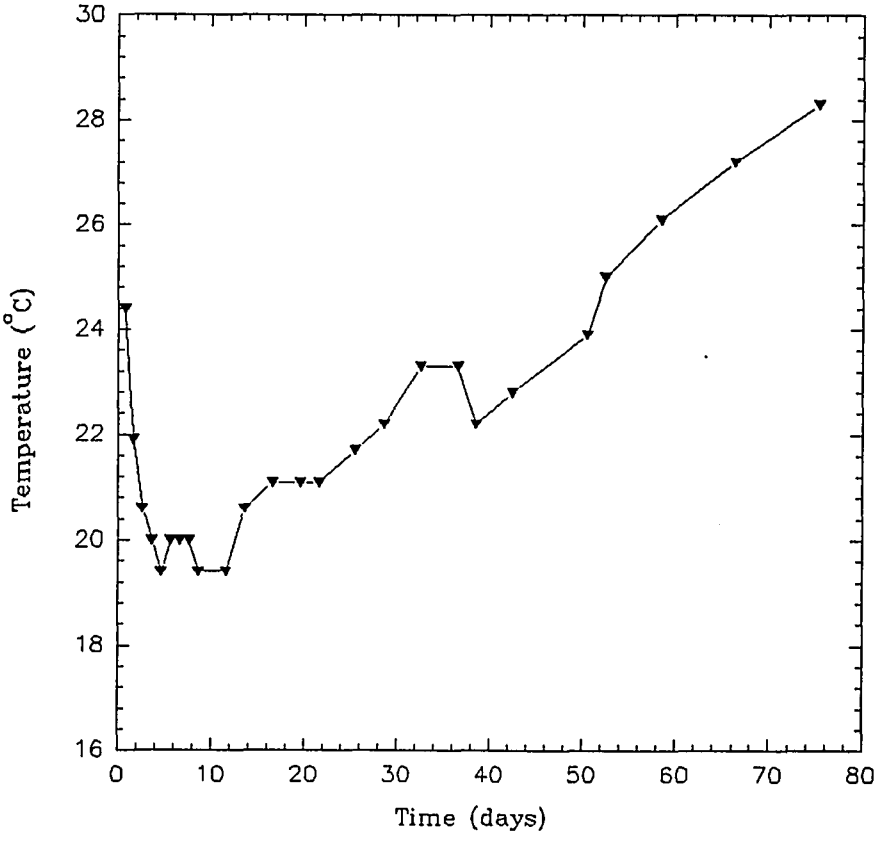


**Figure 5.1: Water Temperature in the Outer Ring**

Other minor effects of temperature increase included changes in viscosity of the water and enhance microbiological growth. Water viscosity is also inversely proportional to temperature, but no corrections were made for this factor. No evidence of excessive microbiological growth, such as a surface slime, were evident when the SDRI was removed.

### Swell Measurements

Because the swell gage was stolen several weeks into the test, swelling of the clay could not be measured. However, the wetting front must be below the level of the inner ring (about 15 cm) for swelling to push the inner ring upward; swelling from a shallower wetting front could not move the inner ring. As discussed in a later section, the wetting front never reached deeper than 4 to 6 cm, and thus swell could not have been measured with the setup provided with the SDRI.

### Infiltration Rate

In general, the infiltration rate curve acted as theory predicted with high initial infiltration rates and a slow approach to the steady state infiltration rate. Figure 5.2 plots infiltration rate (I) against time, and shows the measured data as well as a best fit power curve. Some scatter

occurs in the data, but the high correlation coefficient ($r^2$) indicates that the scatter was insignificant.

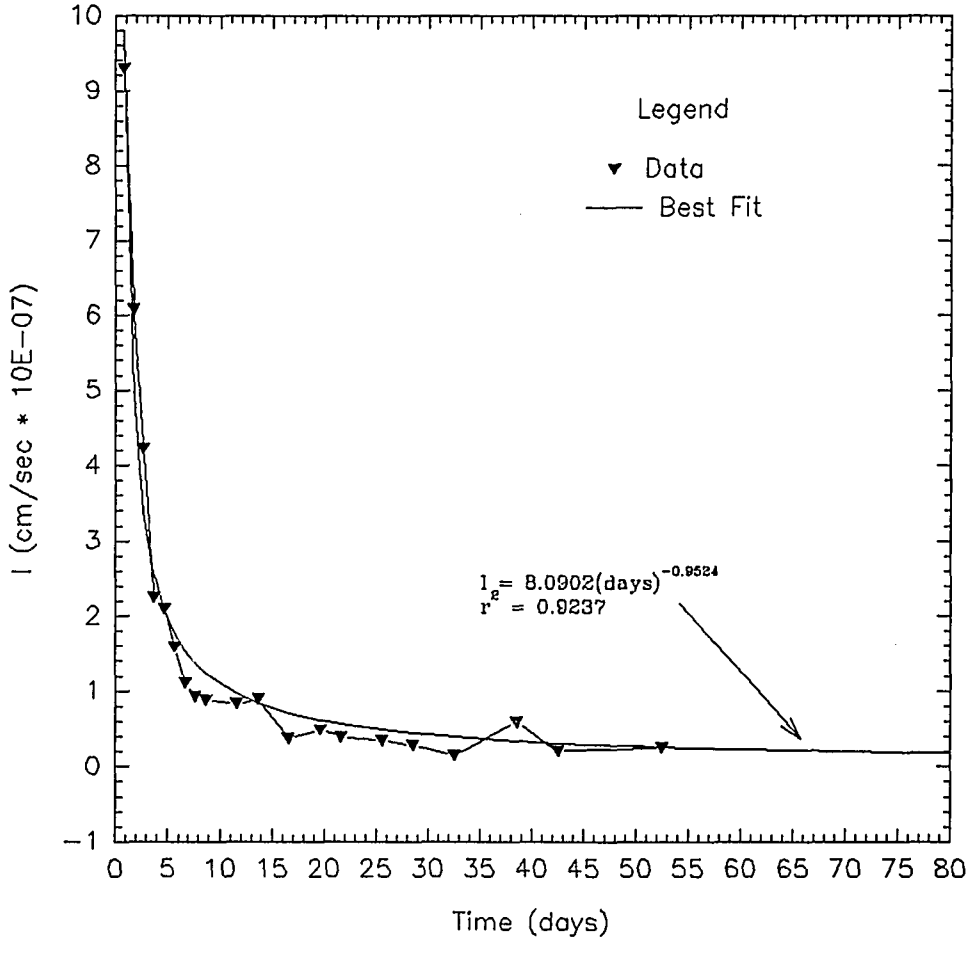


**Figure 5.2: Infiltration Rate vs. Time**

A total of 25 data points were collected over 75.30 days. However, 5 of these points were discarded because the flexible bag weighed more when taken off than when put on, which resulted in illogical negative infiltration rates. Figure 5.2, therefore, reflects only 20 data points collected over 52.48 days. Table A3 in the Appendix shows the raw data and infiltration calculations for all 25 data points.

All of these bad measurements occurred near the end of the test when temperature increased the most and problems with purging air from the inner ring occurred. Air in the inner ring could be from several sources: dissolved gases leaving solution, biological activity, or entrapped air that escaped from below the wetting front. In any case, accumulations of air in the inner ring could force water out of the inner ring and back into the flexible bag. Attempts were made to purge the air by opening the flush tube and tapping the inner ring, but it was difficult to be sure all air was removed.

In order to calculate $K_{sat}$, the steady state infiltration rate must be estimated from the measured data. An average of the last five good data points, which more or less represent the flattest part of the infiltration curve, yielded a steady state infiltration rate of $2.98 \times 10^{-8}$ cm/sec.

## Identifying the Wetting Front

The condition and nature of compacted clay made identification of the wetting front difficult. The clay was approximately 90% saturated during construction and therefore the difference in water content between the wetting front and background was only about 10% of the porosity. Moreover, a wetting front in compacted clay will be diffuse rather than sharp. Both factors led to difficulties in detecting and defining the wetting front.

Because the clay pad was not instrumented to detect a shallow wetting front, direct physical evidence of the depth of the wetting front was lacking. Nonetheless, two pieces of physical evidence point to a reasonable estimate of the depth of the wetting front. First, the dye tracer (FD&C Green #3) stopped uniformly at a depth of about 2 cm. Because this dye is cationic, it sorbed strongly and the wetting front therefore must have been in advance of the dye front. This conclusion was supported by the findings of Elsbury et al. (1990) and DBS&A (1991) as discussed in Chapter 2, Literature Reviewed.

The TDR water content profiles collected when the SDRI was removed provided the strongest evidence, although the scatter in the data prohibited conclusively establishing the depth of

the wetting front. In general, the four water content profiles showed a trend of a nearly saturated zone near the pad surface, a drier zone between about 3 and 7 cm, and then increasing water content to another nearly saturated zone below 15 or 20 cm. Downward redistribution of the water added during construction may have produced this trend, or the bottom lifts may have been laid wetter than the upper lifts.

Two of the four profiles (#1 and #2) exhibited a distinct dry zone between 3 and 6 cm. Profile #4 did not show a dry zone at those depths and profile #3 showed a dry area intermediate between profiles #3 and #1. In any case, the wetting front cannot have reached the dry zone and a reasonable estimate of the depth of the wetting front would be between 4 and 6 cm.

Figure 5.3 summarizes the dye and water content data and shows the estimated depth of the wetting front. All further calculations were based on a wetting front depth of 4 cm, although the choice between 4 and 6 cm was arbitrary. The uncertainty introduced into $K_{sat}$ by this choice will be discussed in a later section of this chapter.

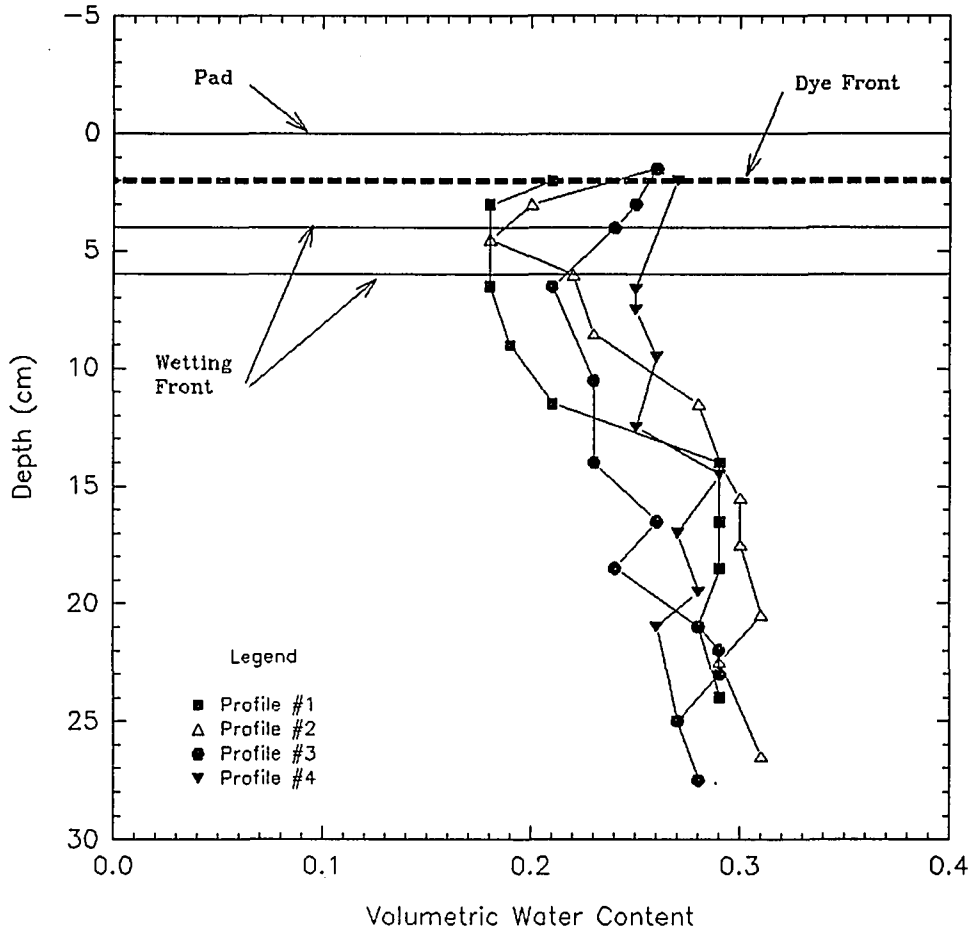


**Figure 5.3: Identifying the Wetting Front**

## Hydraulic Gradient

As shown in Equation 4.6 (Chapter 4, Data Reduction), the hydraulic gradient is dependent on the depth of water in the outer ring, the depth of the wetting front, and the suction head at the wetting front. The best estimate of the depth of the wetting front was discussed in the previous section; the other two components will now be discussed.

Depth of Water in the Outer Ring

The depth of water in the outer ring (H) was time-averaged as explained in Chapter 4, Data Reduction (see Table A2, Appendix). The resulting value of D was 29.94 cm, based on 25 measurements over 75.28 days.

Wetting Front Pressure Head

Unlike computing the depth of water in the outer ring and estimating the depth of the wetting front, calculating the suction head (negative pressure head) at the wetting front was not straight forward. In fact, this parameter can be estimated in at least three ways. Trautwein suggested two methods as follows:

1) assume $H_s = 0$.
2) assume $H_s = H_i$; where $H_i$ is the ambient suction in the soil below the wetting front.

For this study, the ambient suction ahead of the wetting front was estimated from the tensiometer data. The average of the last five non-zero readings from the four functioning tensiometers was considered representative of the ambient suction. Earlier suction head values were not used because suction head decreased throughout the 75 day test and those values would not correspond to final infiltration rate. The resulting ambient suction head was -65.6 cm.

A third method to estimate $H_s$ was the air entry value for the clay, which is equivalent to the height of capillary rise. Using the soil moisture release curve developed by DBS&A using Van Genuchten's method, the air entry value was estimated as -500 cm, as shown in Figure 5.4.

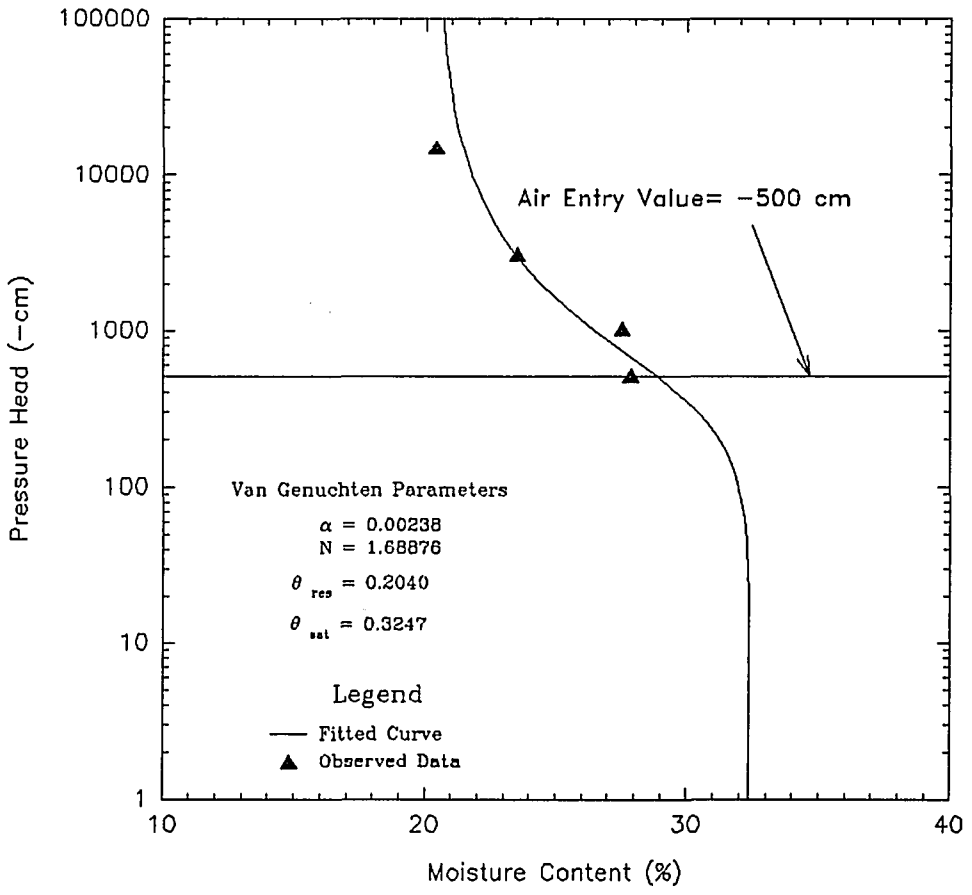


**Figure 5.4: Soil Moisture Release Curve and Air Entry Value (provided by DBS&A)**

The air entry value could have been chosen anywhere from -100 to -500 cm, but the greater tension was chosen in order to produce the maximum range of hydraulic gradients. Depending on the assumptions and methods chosen, three different but equally valid estimates of wetting front suction head can be used to calculate $K_{sat}$. Table 5.3 summarizes the different values produced in this project.

Table 5.3

Wetting Front Suction Head

| Method or Assumption | Head (cm) |
|---|---|
| $H_s = 0.0$ | 0.0 |
| $H_s = H_i$ = ambient suction head | -65.6 |
| $H_s = H_c$ = air entry value | -500 |

Hydraulic Gradient

Two parts of the hydraulic gradient, the depth of the water in outer ring and the depth of the wetting front, had a single best estimate in this study. Because the third component of the hydraulic gradient, the wetting front suction head, can have 3 values depending on assumptions, the resulting hydraulic gradient can also have 3 values. Table 5.4 compiles the three estimates of the hydraulic gradient.

Table 5.4

Hydraulic Gradient (i)

| Method or Assumption | i (cm/cm) |
|---|---|
| $H_s = 0.0$ | 8.5 |
| $H_s = H_i$ = ambient suction head | 24.9 |
| $H_s = H_c$ = air entry value | 133 |

## Saturated Hydraulic Conductivity ($K_{sat}$)

The saturated hydraulic conductivity was calculated by dividing the steady state infiltration rate by the hydraulic gradient as shown below:

$$K_{sat} = \frac{I_{ss}}{i} \qquad (5.1)$$

where: $K_{sat}$ = saturated hydraulic conductivity (cm/sec)
$I_{ss}$ = steady state infiltration rate (cm/sec)
i = hydraulic gradient (dimensionless)

As with the hydraulic gradient, three values of $K_{sat}$ were possible depending on how the head at the wetting front was estimated. Table 5.5 summarizes the estimates of steady state infiltration rate ($I_{ss}$), hydraulic gradient (i), and saturated hydraulic conductivity ($K_{sat}$).

**Table 5.5**

**Saturated Hydraulic Conductivity ($K_{sat}$)**

| Method or Assumption | $I_{ss}$ (cm/sec) | i (cm/cm) | $K_{sat}$ (cm/sec) |
|---|---|---|---|
| $H_s = 0.0$ | $2.98 \times 10^{-8}$ | 8.5 | $3.5 \times 10^{-9}$ |
| $H_s = H_i$ | $2.98 \times 10^{-8}$ | 24.9 | $1.2 \times 10^{-9}$ |
| $H_s = H_c$ | $2.98 \times 10^{-8}$ | 133 | $2.2 \times 10^{-10}$ |

Increasing $H_s$ (i.e., greater suction) led to higher hydraulic gradients and decreasing $K_{sat}$. Clearly the test pad passed the $10^{-7}$ cm/sec federal standard for hydraulic conductivity, even with about one order of magnitude variation due to the choice of $H_s$. Uncertainty in the depth of the wetting front, as discussed in a previous section, caused roughly 50% variation in $K_{sat}$, but in no case caused an order of magnitude variation. For example, if the wetting front were 6 cm deep, $K_{sat}$ would be $5.0 \times 10^{-9}$, $1.8 \times 10^{-9}$, and $3.3 \times 10^{-10}$ cm/sec for $H_s$ of 0, -65.6, and -500 cm, respectively.

Which estimate of $K_{sat}$ is "best"? The answer depends largely on how the estimate will be used. For permitting purposes, the $K_{sat}$ based on $H_s = 0.0$ would predict the greatest leakage, and therefore would be the most conservative and most appropriate. For scientific purposes, $K_{sat}$ based on the $H_s$ of

the air entry value may be the most accurate. However, air entry values from core samples may differ from the air entry value of the pad for the same reasons that laboratory and in-situ $K_{sat}$ may differ. In any case, the method of estimating $H_s$ must be known for valid comparisons between studies.

Table 5.6

**Comparison of Laboratory and SDRI Values of $K_{sat}$ (all values in cm/sec)**

| Laboratory Tests | | SDRI | |
|---|---|---|---|
| Flexible Wall, Undisturbed Cores (WT) | $1x10^{-7}$ $3x10^{-8}$ | $H_s$=0. cm | $3.5x10^{-9}$ |
| Flexible Wall, Recompacted Core (DEE) | $1.3x10^{-9}$ | $H_s$=-65.6 cm | $1.2x10^{-9}$ |
| Falling Head, Undisturbed Core (DBS&A) | $2.5x10^{-8}$ | $H_s$=-500 cm | $2.2x10^{-10}$ |

WT = Western Technologies, Inc.
DEE = Desert Earth Engineering, Inc.
DBS&A = Daniel B. Stephens and Assoc., Inc.

Table 5.6 compares the laboratory and SDRI values of $K_{sat}$. The SDRI values of $K_{sat}$ were lower than the laboratory values by about two orders of magnitude, with the exception of the laboratory $K_{sat}$ from the recompacted core. However,

recompaction probably results in a core unlike the test pad or the other core samples, and thus the agreement between the recompacted sample $K_{sat}$ and the SDRI $K_{sat}$ was accidental. Because the laboratory tests were performed by outside consultants, details of the tests were not known and it was impossible to tell if laboratory conditions were similar to field conditions. If high pressures were combined with inadequate side wall pressure or sealing, the flexible wall tests could have overestimated laboratory $K_{sat}$.

These results also suggested that preferential flow was not significant in the test pad at Page Ranch. According to current thinking, the small samples used in laboratory tests miss preferential flow and thus underpredict $K_{sat}$. The uniformity of the dye front showed that preferential flow had not occurred, at least in the top 2 cm. Moreover, if preferential flow had occurred, it would be unlikely that the SDRI values of $K_{sat}$ would be lower than the laboratory values.

Most other studies that compared laboratory and in-situ (not necessarily from SDRIs) values of $K_{sat}$ found just the opposite -- laboratory $K_{sat}$ was lower than in-situ $K_{sat}$ (Daniel, 1981; Daniel, 1984; Day and Daniel, 1985; Rogowski, 1986). Two studies (Trautwein and Daniel, 1986; Elsbury, 1990) that

did compare SDRI and laboratory results showed that SDRI values fell within the range of laboratory values.

In the debut test of an SDRI, Trautwein and Daniel (1986) showed that the SDRI $K_{sat}$ of $8x10^{-8}$ cm/sec was within the range of $10^{-7}$ to $10^{-8}$ cm/sec from laboratory tests. Suction head at the wetting front was not considered and therefore their SDRI $K_{sat}$ was a maximum value. The laboratory tests were conducted with a flexible wall permeameter.

Elsbury (1990) likewise found that four SDRIs yielded a range of $K_{sat}$ from $1x10^{-4}$ to $3x10^{-5}$ cm/sec, which fell within the rather wide range of laboratory values from $10^{-3}$ to $10^{-9}$ cm/sec. Suction head at the wetting front was not a concern because steady state outflow was established from the bottom of the one foot thick pad.

In summary, $K_{sat}$ values from SDRIs can be considered only order of magnitude estimates unless the treatment of suction at the wetting front is known. Furthermore, laboratory values are not necessarily lower than in-situ values. Although this thesis was not intended to investigate the different types of

laboratory tests, it is clear that laboratory testing must be designed with care if results are to be accurate predictors of field conditions.

## Pore Water Velocities

Pore velocities were calculated by two methods: 1)using the measured depth of the wetting front and the elapsed time of the test (Eqn. 5.2), and 2) Darcy's law (Eqn. 5.3). Regardless of the calculation method, the result was an average linear velocity based on measurable macroscopic terms. The true microscopic velocities are generally larger than the average linear velocity because the water particles must travel along irregular paths that are longer than the linearized path represented by the average linear velocity (Freeze and Cherry, 1979). Table 5.6 shows the results of the calculations based on wetting front depths of 4 and 6 cm for the first approach, and based on the three choices of $H_s$ for the second approach.

$$\bar{v} = \frac{\textit{depth of wetting front}}{\textit{elapsed time}} \qquad (5.2)$$

where: $\bar{v}$ = average linear velocity (cm/sec)
depth of wetting front = 4 or 6 cm
elapsed time = 75.30 days = 6,505,920 sec

$$\bar{v} = \frac{Q}{(\eta - \theta_{res})A} = \frac{v}{\eta - \theta_{res}} = \frac{K_{sat}}{\eta - \theta_{res}}\ (i) \qquad (5.3)$$

where: Q = volumetric flux ($cm^3/sec$)
A = cross sectional area ($cm^2$)
v = specific discharge (cm/sec)
$\bar{v}$ = average linear velocity (cm/sec)
$\eta$ = porosity = 0.29 $cm^3/cm^3$
$\theta_{res}$ = residual water content = 0.20 $cm^3/cm^3$
$\eta - \theta_{res}$ = effective porosity ($cm^3/cm^3$)
i = hydraulic gradient (dimensionless)
Ksat = saturated hydraulic conductivity (cm/sec)

Table 5.7

Pore Water Velocities

| Depth/Time (cm/sec) | | Darcy Velocity (cm/sec) | |
|---|---|---|---|
| depth=4 cm | $6.2 \times 10^{-7}$ | $H_s$=0. cm | $3.3 \times 10^{-7}$ |
| depth=6 cm | $9.2 \times 10^{-7}$ | $H_s$=-65.6 cm | $3.3 \times 10^{-7}$ |
| | | $H_s$=-500 cm | $3.2 \times 10^{-7}$ |

## Bromide Tracer Results

A total of 16 bromide profiles were established from clay samples taken from the inner ring when the SDRI was dismantled. Four of these profiles extended to 20 cm at 2 cm depth intervals, while the other 12 profiles went to 10 cm depth at 2 cm intervals. Sample collection, bromide extraction, bromide measurement with an ion chromatograph, and data reduction are discussed in detail in Chapters 3 and 4.

Figure 5.5 depicts the four profiles that extended to 20 cm and illustrates the amount of scatter in any single profile. As discussed in Chapter 4, Data Reduction, the average error in these concentrations was about ±1.4 mg/l. The largest cause of error was the average dilution factor used to

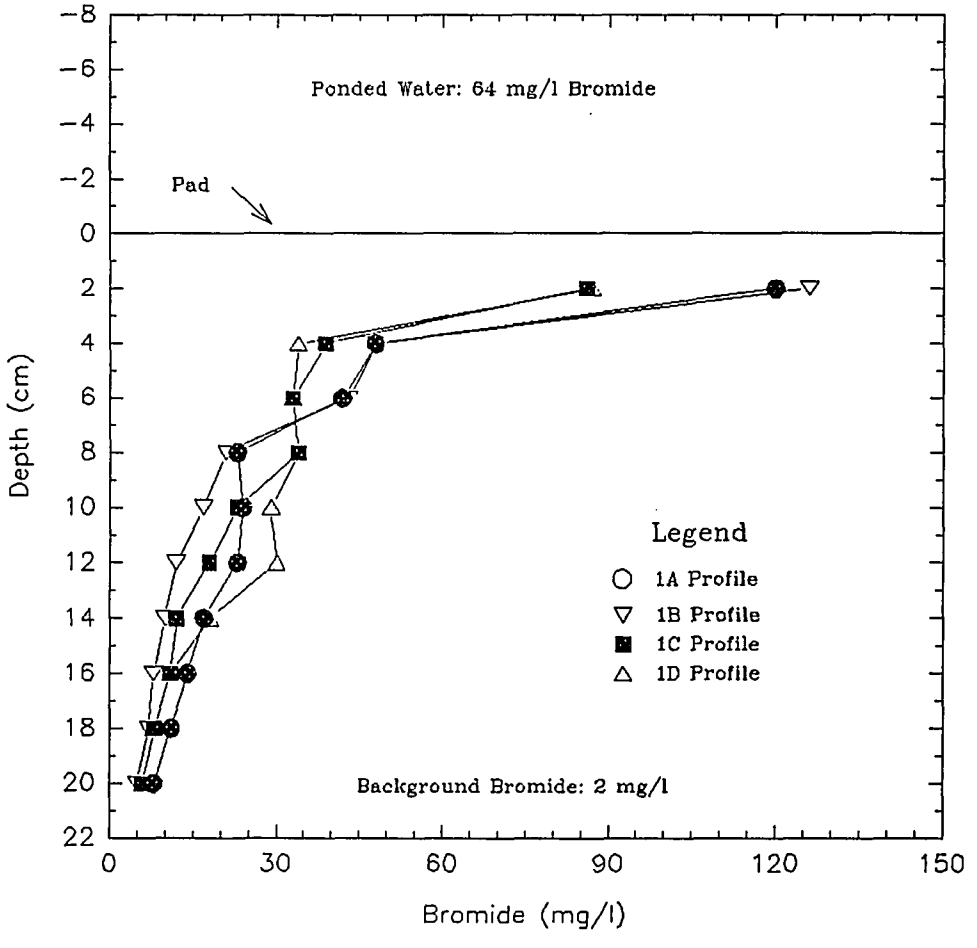


**Figure 5.5: Four Bromide Profiles**

calculate concentrations. Increased water content sampling would have provided a more accurate dilution factor and perhaps permitted varying the dilution factor with depth.

All sixteen profiles are interpreted in Figure 5.6 in light of possible transport mechanisms. Bromide concentrations at 2 cm depth were higher than either the source concentration or concentrations deeper in the pad. Two possible explanations, neither of which could be proved or disproved, were:

1) Evaporative concentration of bromide near the surface of the pad during the afternoon when the SDRI was drained and the next morning when the clay was sampled. Although the pad was covered with plastic during this period, some evaporation surely occurred.

2) Interactions between the clay, the cationic dye, and the bromide may have caused the dye to accumulate near the surface. Laboratory tests would be needed to determine the sorption of bromide under these conditions.

In the first scenario, the high bromide calculations would be a figment of an error in the dilution factor because the original water content was not known. In the second scenario, the high bromide concentrations would reflect a real

accumulation of bromide, even though bromide is usually considered a non-reactive tracer. Both factors may have contributed, but it seemed more likely that evaporative concentration was the cause even though it could not be proved.

In any case, advection carried bromide to a depth of 4 to 6 cm, based on the depth of the wetting front established previously in this chapter. Below the wetting front, diffusion moved bromide another 14 to 16 cm to a depth of 18 or 20 cm where background bromide levels occurred.

Theoretical diffusion profiles based on Crank's one dimensional solution of Fick's second law (Freeze and Cherry, 1979) are also shown in Figure 5.6. Calculations are compiled in Table A10 in the appendix, but note that the initial concentration was 64 mg/l, the time was 75.3 days, and the average volumetric water content was 0.26. Recall that the free solution diffusion coefficient ($D_o$) is multiplied by tortuosity to yield the effective diffusion coefficient ($D^*$), but that tortuosity is not directly measurable and may lump together the effect of other factors such as anion exclusion (Shackelford and Daniel, 1991a).

This approach was somewhat simplified from reality because it assumed that the wetting front was a constant source in time and position, and that diffusion began at the end of the wetting front. In reality, downward advection and diffusion

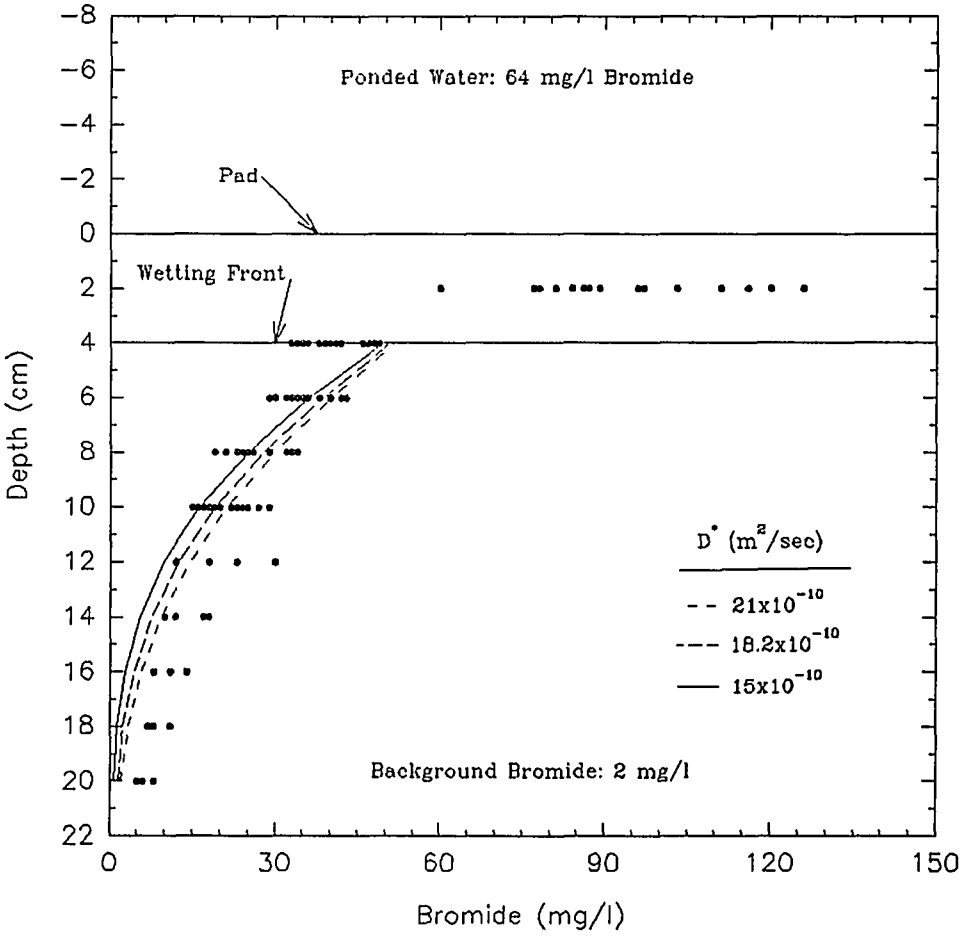


**Figure 5.6: Theoretical and Measured Bromide Diffusion Profiles**

proceeded concurrently with time from the surface of the pad. In defense of this approach, however, it was intended only as a "back of the envelope check" to see if diffusion could account for bromide movement on the order of 14 to 16 cm.

Three different diffusion curves are shown for a range of $D^*$ (effective diffusion coefficient) from $15x10^{-10}$ to $21x10^{-10}$ $m^2/sec$. The intermediate value of $18.2x10^{-10}$ $m^2/sec$ was published by Shackelford (1989) for a smectite clay. Although Shackelford derived this value from a reservoir diffusion test, he was not able to verify it by curve fitting to a diffusion profile. Nonetheless, it was more appropriate for this analysis than other values for kaolinite clays because the Atterberg limits indicated that the clay at Page Ranch was composed of montmorillonite and illite. The value of $21x10^{-10}$ $m^2/sec$ is the diffusion coefficient in free solution ($D_o$) and therefore that curve represents the theoretical maximum rate of diffusion.

Concentrations were underpredicted at depth and slightly overpredicted near the wetting front, but in general the theoretical curves overlapped the observed data. If the wetting front were deeper, the curves would be shifted down

and to the right (relative to the observed data), and would better match the observed data at depth.

As far as this author could determine, there were no other field studies in compacted clay for comparison of the depth of bromide diffusion. To simply illustrate the amount of possible diffusion, however, Johnson et al. (1989) found that chloride diffused a maximum of 83 cm in 5 years into a natural clay layer beneath a landfill in Ontario.

In order to look at possible preferential flow, the bromide profiles were plotted as five contour maps for depths of 2, 4, 6, 8, and 10 cm (see Figures 5.7 to 5.11). The accuracy of the bromide data (±1.4 mg/l) was near or greater than the contour interval in Figures 5.8, 5.9, 5.10, and 5.11.

Figures 5.7, 5.8, and 5.9 consistently show high bromide concentrations in the northeast (upper left) corner, but Figures 5.10 and 5.11 show low concentrations in the northeast (upper left) corner. Although this data suggested a lift interface between 6 and 8 cm, the construction documentation was not detailed enough to verify a lift interface at that depth.

No other trends were apparent in the bromide contour plot, which suggested that preferential flow was insignificant in the test pad. Given that the wetting front was quite shallow, preferential flow would have been hard to discern even if it had occurred. "Preferential diffusion" was not mentioned anywhere in the literature, and would only make sense in terms of anion exclusion. In closing, note that as a test pad for a proposed cover at Page Ranch, transport of ions was more of an academic concern than a possible problem.

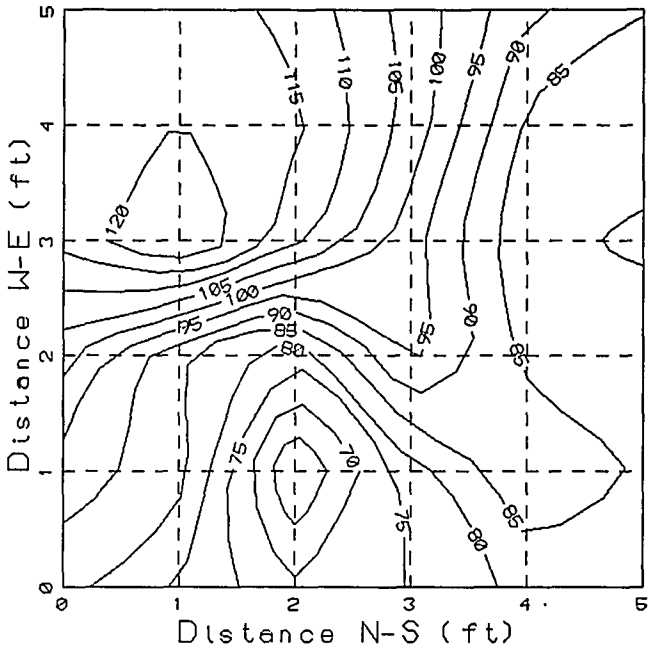


**Figure 5.7: Bromide Contour Plot at 2 cm Depth**
(Concentrations in mg/l)

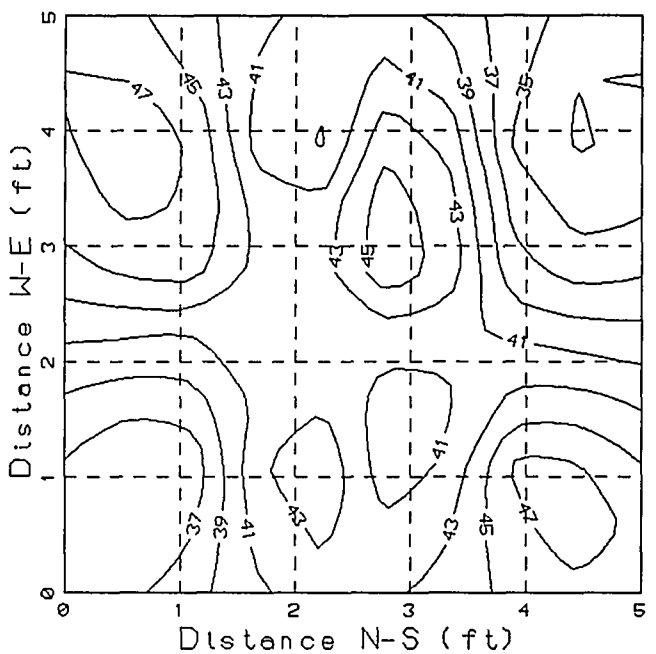


**Figure 5.8: Bromide Contour Plot at 4 cm Depth**
(Concentrations in mg/l)

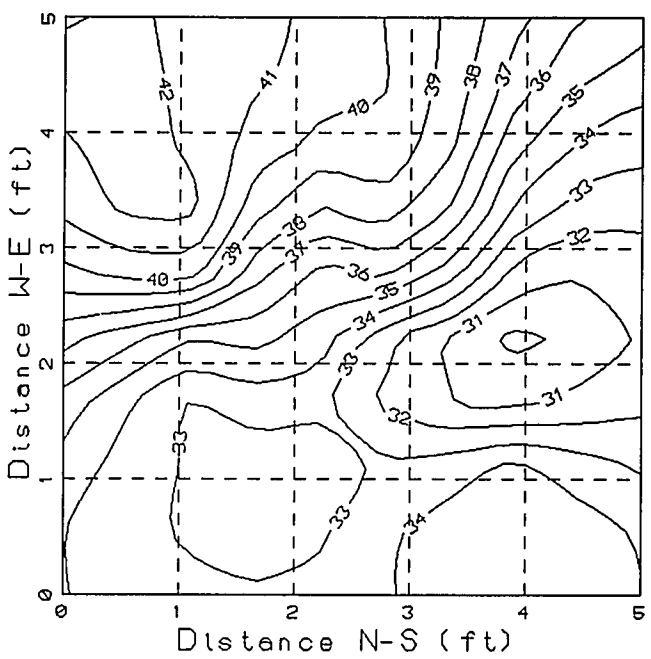


**Figure 5.9: Bromide Contour Plot at 6 cm Depth**
(Concentrations in mg/l)

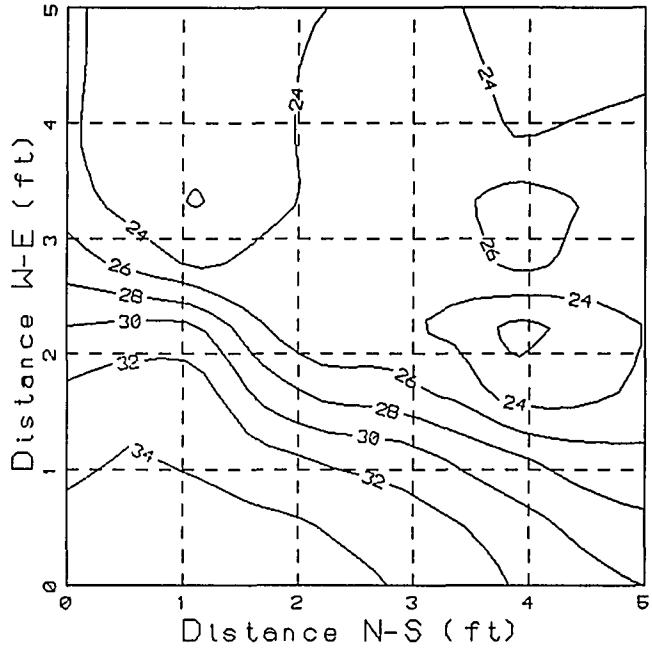


**Figure 5.10: Bromide Contour Plot at 8 cm**
(Concentrations in mg/l)

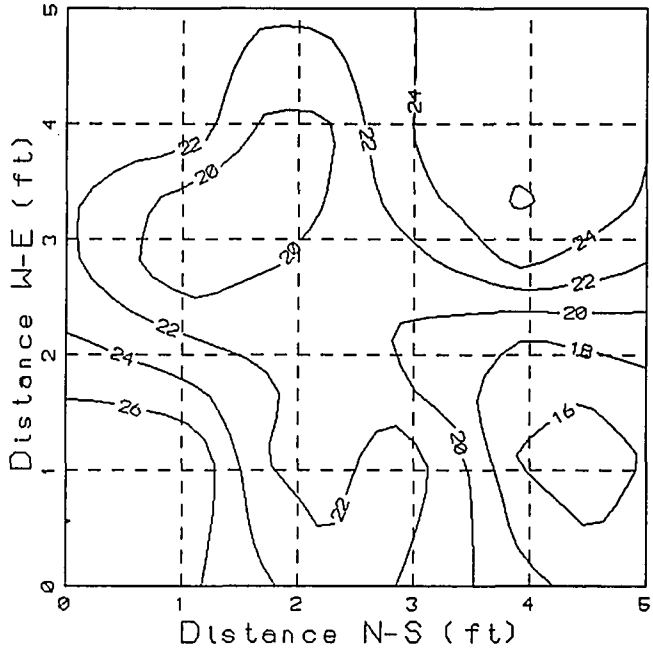


**Figure 5.11: Bromide Contour Plot at 10 cm**
(Concentrations in mg/l)

# CHAPTER 6

## SIMULATION OF THE WETTING FRONT

The purpose of this simulation was to evaluate if the computer model PICARD could predict the observed wetting front. Because calibration or verification of the model was not a goal, only one set of input parameters, the best estimates from the results, was used to model the wetting front.

The program PICARD solves the one-dimensional Richard's equation with either prescribed heads or flux boundary conditions by using the Galerkin finite element method. The finite element formulation can be found in Khaleel and Yeh (1985). The program has been modified since that original paper to include automatic time stepping, vertical or horizontal flow, and variably saturated flow in homogenous or heterogenous soils.

Transient, vertical flow was simulated through a 20 cm deep profile of a single soil type (i.e., compacted clay) using twenty cells (1 cm length) and 21 nodes; unsaturated soil parameters were represented by the Van Genuchten model (1980). A time step of 30 seconds was used over the total test time of 75 days and results were output at 15, 30, 45, 60, and 75 days. The maximum number of 25 iterations was used with the

Picard scheme and the tolerance was 0.1. Table 6.1 compiles the soil properties and boundary conditions for PICARD.

**Table 6.1**

**Input Parameters for PICARD**

| Parameter | Quantity |
|---|---|
| $K_{sat}$ | 5 x $10^{-9}$ cm/sec |
| $\alpha$ | 0.00238 |
| N | 1.6888 |
| Saturated water content ($\theta_{sat}$) | 0.3247 $cm^3/cm^3$ |
| Residual water content ($\theta_{res}$) | 0.2040 $cm^3/cm^3$ |
| Upper fixed head boundary ($\psi$) | 29.94 cm |
| Lower fixed head boundary ($\psi$) | -1200 cm |
| Initial head in profile ($\psi$) | -1200 cm |

The $K_{sat}$ of 5 x $10^{-9}$ cm/sec was chosen as conservative (i.e., high) value based on the SDRI results of 3.5 x $10^{-9}$ to 2.2 x $10^{-10}$ cm/sec. The Van Genuchten parameters were supplied by DBS&A and were based on testing one core sample. Although the saturated water content of that one core sample was higher than the average saturated water content (porosity) of 0.29 estimated from other core samples taken throughout the project (see Table 5.2), it was only slightly higher than the range of saturated water contents of 0.27 to 0.31 (again, see Table 5.2).

The fixed upper head boundary was simply the time averaged head in the outer ring. Initial conditions and the fixed lower head boundary of -1200 cm corresponded to the matric potential at the average volumetric water content of 0.26 (see Table 5.2) as read from the soil moisture release curve provided by DBS&A (see Figure 5.4).

The results of the simulation are presented in Figures 6.1 and 6.2; the model output is included in the Appendix. Figure 6.1, which depicts the change in matric potential ($\psi$) vs. depth below the pad surface, shows that at the end of the 75 day test the predicted wetting front was between 3 and 8 cm. Because the wetting front was inherently diffuse, the wetting front was defined broadly between 0 and -100 cm of matric potential ($\psi$).

Figure 6.2 depicts simulated changes in volumetric water content ($\theta$) vs. depth below the pad surface. Saturated or nearly saturated conditions (i.e., volumetric water content of 0.32 or greater) were predicted to a depth of about 8 cm after 75 days, again indicating the wetting front.

The model was not very sensitive to time -- any time from 15 to 75 days would predict a wetting front that generally agreed with the observed data. By visualizing curves for greater

time periods, say 90 or 105 days, it appeared that even these wetting fronts would generally agree with the observed data. In short, PICARD predicted very little flow in the compacted clay, but that in itself could be viewed as a success.

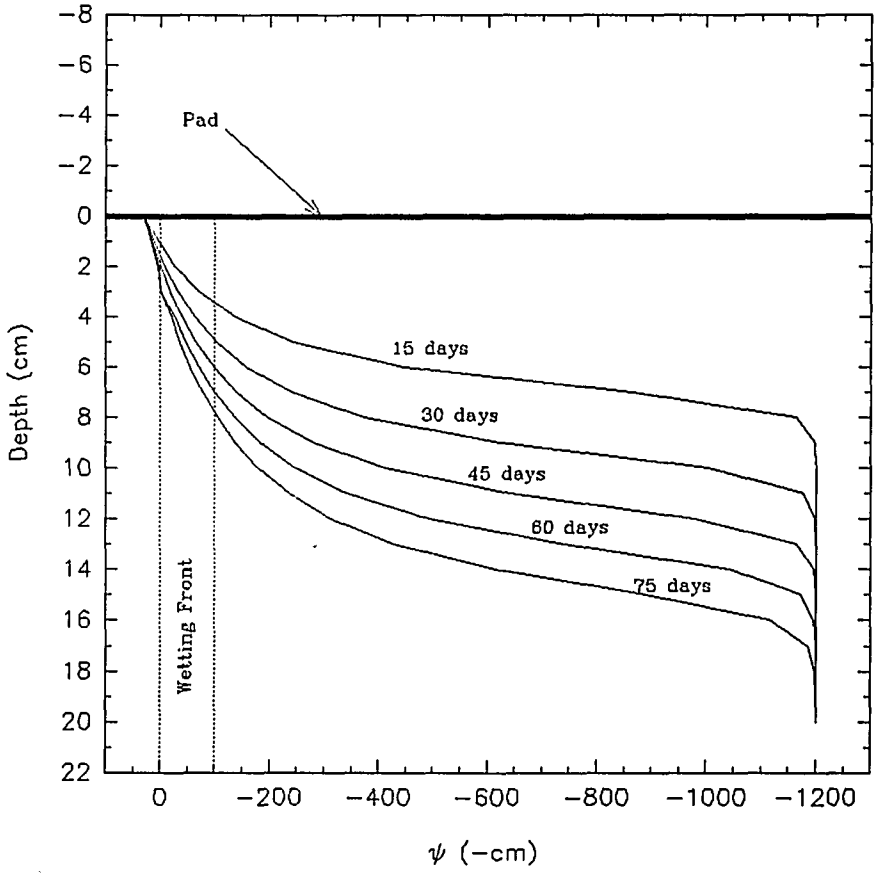


**Figure 6.1: Simulated Wetting Front ($\psi$ vs Depth)**

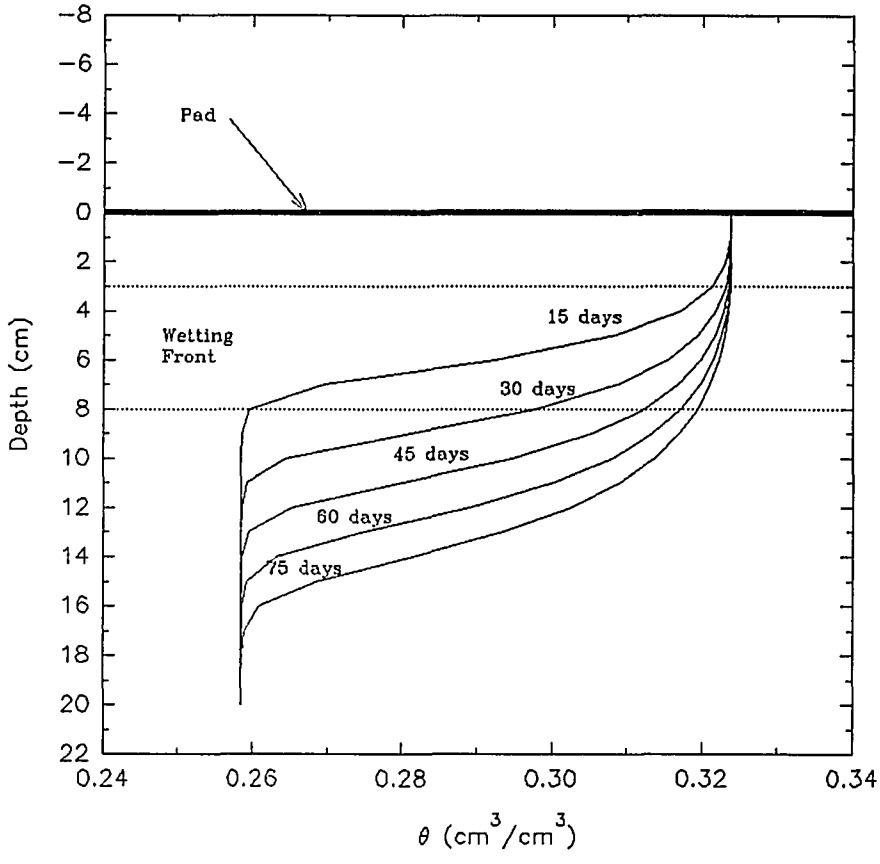


**Figure 6.2: Simulated Wetting Front ($\theta$ vs. Depth)**

The simulated wetting front of 3 to 8 cm agreed surprisingly well with the observed wetting front of 4 to 6 cm. However, this agreement cannot be considered conclusive because the observed wetting front was inferred from dye and bromide tracer data rather than measured directly by water content and/or matric potential changes. Furthermore, the model was not sensitive to time (as previously discussed).

Although the ability of PICARD to predict the wetting front was encouraging, part of this success must be attributed to the observed lack of preferential flow in the test pad. The code did not model preferential flow, and if preferential flow had been significant, the model would have underpredicted the wetting front. For this reason, modelling based on soil and hydraulic properties from core samples that may exclude preferential flow paths must be viewed with caution.

In summary, PICARD was able to predict the wetting front in compacted clay and this success was in part due to the lack of preferential flow in the test pad. Modelling cannot replace in-situ testing unless preferential flow can be included in the model, and even then in-situ testing would be desirable to calibrate and verify the model.

# CHAPTER 7

# CONCLUSIONS AND RECOMMENDATIONS

## Conclusions

Saturated hydraulic conductivity ($K_{sat}$) from the SDRI test varied from $3.5 \times 10^{-9}$ to $2.2 \times 10^{-10}$ cm/sec depending on the treatment of suction head at the wetting front. Because the choice of suction head at the wetting front can cause an order of magnitude variation in $K_{sat}$, caution must be used when comparing results from different studies.

SDRI values of $K_{sat}$ were approximately one order of magnitude lower than the laboratory values of $10^{-8}$ to $10^{-9}$ cm/sec. Undisturbed cores yielded laboratory values of about $10^{-8}$ cm/sec, whereas a recompacted core yielded a $K_{sat}$ of about $10^{-9}$ cm/sec. The small sample size used for laboratory testing was an inherent reason for a discrepancy that usually produces laboratory $K_{sat}$ less than in-situ $K_{sat}$, but in this case the large volume sampled by the SDRI yielded a lower $K_{sat}$.

Although the pad was not instrumented to detect a shallow wetting front, the dye front and water content data indicated that the wetting front penetrated 4 to 6 cm in the 75 day

test. The cationic dye (FD&C green #3) was strongly sorbed by the clay and only penetrated 2 cm.

Comparing theoretical bromide diffusion profiles to the data suggested that bromide could move by diffusion 14 to 16 cm below the wetting front. The fit was not exact, however, with greater bromide concentrations at depth than predicted by the theoretical profiles. Even with uncertainties in the dilution factor for back calculating bromide concentrations and the limitations of the approach, the data did confirm that diffusion was an important mode of transport in the compacted clay.

As fit by eye, the effective diffusion coefficient ($D^*$) was on the order of 15 to $20.8 \times 10^{-10}$ $m^2/sec$, with $20.8 \times 10^{-10}$ $m^2/sec$ being the free solution diffusion coefficient ($D_o$). The $D^*$ from this study matched a published value of $18.2 \times 10^{-10}$ $m^2/sec$ for another smectite clay (Shackelford et al., 1989). These high $D^*$ values suggested that anion exclusion may be important for bromide diffusion in smectites.

The uniformity of the dye and bromide fronts suggested that preferential flow was insignificant in the test pad, although the lack of documentation of lift heights made interpretation

difficult. No cracks or lift interfaces were visible when the pad was dissected.

The test clay pad met the federal standard of $10^{-7}$ cm/sec for hydraulic conductivity. Although the tracer results were scientifically interesting, they were of little practical importance because the test was for a proposed cover -- all waste will be below the clay and upward transport will not be a concern.

The unsaturated flow program PICARD predicted a wetting front of 3 to 8 cm that agreed well with the observed wetting front of 4 to 6 cm. Part of this agreement must be attributed to the observed lack of preferential flow in the test pad given that PICARD does not model preferential flow.

## Recommendations

Given the clear vision of hindsight, some of the SDRI test procedures should be revised. The following changes are recommended:

- The SDRI test should not be conducted over a change in season in order to minimize temperature changes. Water density, viscosity, the amount of dissolved gases in the water, and the size of the inner ring all change with temperature.

- Some sort of pump to purge air from the inner ring is needed. Tapping the inner ring with a broom handle to dislodge air bubbles was tedious, and may or may not have been effective.

- More thought should be put into dye selection. The cationic dye (FD&C Green #3) was quickly sorbed by the clay and therefore provided little information. Moreover, it may have reacted with the bromide tracer, although laboratory tests would be necessary to prove or disprove this possible reaction.

- The ion specific probe that was first used to monitor bromide concentrations did not yield precise or accurate data, most likely due to interferences from other ions. An ion chromatograph yielded bromide measurements that were accurate to ±0.1 mg/l.

- Construction should be well documented, especially lift interfaces, in order to interpret dye and tracer data.

- The pad should be instrumented to identify shallow as well as deep wetting fronts, and if possible to track wetting front movement. For example, thermocouple psychrometers, soil moisture blocks, and tensiometers would cover a wide range of water content conditions.-

- In-situ water content is important for several reasons: 1) it is the largest source of error in the dilution factor used to back calculate bromide concentrations from clay samples, 2) it is a source of error in the calculation of theoretical diffusion profiles in unsaturated conditions, 3) it is probably the best method to track or identify a wetting front. If TDR is used, Topp's regression equation (1980) should be verified for use in compacted clay.

- Clay samples for tracer analysis should be collected as soon as possible after draining the SDRI to prevent evaporative concentration of the tracer near the surface of the pad.

# APPENDIX

| TABLE A1: TENSIOMETER DATA | | | | | | | | | | |
|---|---|---|---|---|---|---|---|---|---|---|
| Date | Time | Days | No. 1 (cb) | No. 1 (cm) | No. 2 (cb) | No. 2 (cm) | No. 4 (cb) | No. 4 (cm) | No. 5 (cb) | No. 5 (cm) |
| 04/25/91 | 09:46 | 0.00 | 30 | -245 | 30 | -234 | 30 | -234 | 0 | 71 |
| 04/26/91 | 08:50 | 0.96 | 30 | -245 | 42 | -357 | 36 | -296 | 0 | 71 |
| 04/27/91 | 08:14 | 1.94 | 31 | -255 | 44 | -377 | 37 | -306 | 0 | 71 |
| 04/28/91 | 08:12 | 2.93 | 32 | -265 | 43 | -367 | 38 | -316 | 0 | 71 |
| 04/29/91 | 08:18 | 3.94 | 32 | -265 | 46 | -397 | 39 | -326 | 30 | -234 |
| 04/30/91 | 08:07 | 4.93 | 34 | -285 | 47 | -408 | 41 | -347 | 39 | -326 |
| 05/01/91 | 08:05 | 5.93 | 34 | -285 | 47 | -408 | 41 | -347 | 38 | -316 |
| 05/02/91 | 07:45 | 6.92 | 34 | -285 | 48 | -418 | 42 | -357 | 37 | -306 |
| 05/03/91 | 08:30 | 7.95 | 33 | -275 | 48 | -418 | 40 | -336 | 34 | -275 |
| 05/06/91 | 08:31 | 10.95 | 33 | -275 | 38 | -316 | 44 | -377 | 28 | -214 |
| 05/08/91 | 08:00 | 12.93 | 31 | -255 | 33 | -265 | 44 | -377 | 24 | -173 |
| 05/10/91 | 08:25 | 14.94 | 30 | -245 | 27 | -204 | 44 | -377 | 23 | -163 |
| 05/11/91 | 07:57 | 15.92 | 29 | -234 | 26 | -194 | 43 | -367 | 24 | -173 |
| 05/14/91 | 08:19 | 18.94 | 5 | 10 | 19 | -122 | 41 | -347 | 21 | -143 |
| 05/16/91 | 09:00 | 20.97 | 4 | 21 | 16 | -92 | 38 | -316 | 22 | -153 |
| 05/20/91 | 07:56 | 24.92 | 5 | 10 | 12 | -51 | 33 | -265 | 22 | -153 |
| 05/23/91 | 08:05 | 27.93 | 12 | -61 | 9 | -20 | 30 | -234 | 20 | -132 |
| 05/27/91 | 08:12 | 31.93 | 12 | -61 | 8 | -10 | 26 | -194 | 19 | -122 |
| 05/31/91 | 08:39 | 35.95 | 12 | -61 | 8 | -10 | 24 | -173 | 17 | -102 |
| 06/02/91 | 08:17 | 37.94 | 12 | -61 | 8 | -10 | 24 | -173 | 18 | -112 |
| 06/06/91 | 08:25 | 41.94 | 12 | -61 | 8 | -10 | 24 | -173 | 18 | -112 |
| 06/14/91 | 08:51 | 49.96 | 10 | -41 | 7 | 0 | 20 | -132 | 16 | -92 |
| 06/16/91 | 08:25 | 51.94 | 10 | -41 | 7 | 0 | 20 | -132 | 16 | -92 |

| TABLE A1: TENSIOMETER DATA | | | | | | | | | | |
|---|---|---|---|---|---|---|---|---|---|---|
| Date | Time | Days | No. 1 (cb) | No. 1 (cm) | No. 2 (cb) | No. 2 (cm) | No. 4 (cb) | No. 4 (cm) | No. 5 (cb) | No. 5 (cm) |
| 06/22/91 | 08:13 | 57.94 | 9 | -30 | 9 | -20 | 17 | -102 | 13 | -61 |
| 06/30/91 | 08:08 | 65.93 | 8 | -20 | 7 | 0 | 16 | -92 | 14 | -71 |

Equations for Table A1

$$p_{gauge}(Pa) = p_{gauge}(cb)\, x \frac{1000\ Pa}{1\ cb}$$

$$h = \left( \frac{-p_{gauge}}{\rho g} \right) 100 + \Delta Z_1 + \Delta Z_2$$

$\rho g = 9810\ N/m^2$ *Note*: $(N/m^2 = Pa)$

No. 1-4: $\Delta Z_1 = 0.0348$ m No. 1: $\Delta Z_2 = 0.3080$ m No. 2-4: $\Delta Z_2 = 0.4096$ m

| TABLE A2: TIME-AVERAGED HEAD IN THE OUTER RING | | | | | | | | | |
|---|---|---|---|---|---|---|---|---|---|
| Date/ Time On | Date/ Time Off | Δt (day) | Σt (day) | H On (in) | H Off (in) | Corr. H On (in) | Corr. H Off (in) | Av. H (in) | Weighted H (in-d) |
| 04/24 15:35 | ----- ----- | ----- | ----- | 10.500 | ----- | 12.000 | ----- | ----- | ----- |
| 04/25 10:31 | 04/25 10:05 | 0.77 | 0.77 | 10.250 | 10.250 | 11.750 | 11.750 | 11.875 | 9.154 |
| 04/26 09:26 | 04/26 09:10 | 0.94 | 1.71 | 10.625 | 10.125 | 12.125 | 11.625 | 11.688 | 11.030 |
| 04/27 08:37 | 04/27 08:19 | 0.95 | 2.67 | 10.563 | 10.563 | 12.063 | 12.063 | 12.094 | 11.531 |
| 04/28 08:23 | 04/28 08:19 | 0.99 | 3.65 | 10.500 | 10.500 | 12.000 | 12.000 | 12.032 | 11.881 |
| 04/29 08:40 | 04/29 08:30 | 1.00 | 4.66 | 10.437 | 10.437 | 11.937 | 11.937 | 11.969 | 12.027 |
| 04/30 08:27 | 04/30 08:15 | 0.98 | 5.64 | 10.375 | 10.375 | 11.875 | 11.875 | 11.906 | 11.699 |
| 05/01 08:21 | 05/01 08:11 | 0.99 | 6.63 | 10.375 | 10.375 | 11.875 | 11.875 | 11.875 | 11.743 |

| TABLE A2: TIME-AVERAGED HEAD IN THE OUTER RING | | | | | | | | | |
|---|---|---|---|---|---|---|---|---|---|
| Date/ Time On | Date/ Time Off | Δt (day) | Σt (day) | H On (in) | H Off (in) | Corr. H On (in) | Corr. H Off (in) | Av. H (in) | Weighted H (in-d) |
| 05/02 07:55 | 05/02 07:50 | 0.98 | 7.61 | 10.188 | 10.188 | 11.688 | 11.688 | 11.782 | 11.528 |
| 05/03 08:48 | 05/03 08:40 | 1.03 | 8.64 | 10.250 | 10.250 | 11.750 | 11.750 | 11.719 | 12.085 |
| 05/06 07:48 | 05/06 07:38 | 2.95 | 11.59 | 10.125 | 10.125 | 11.625 | 11.625 | 11.688 | 34.494 |
| 05/08 08:20 | 05/08 08:11 | 2.02 | 13.61 | 10.063 | 10.063 | 11.563 | 11.563 | 11.594 | 23.373 |
| 05/10 09:00 | 05/10 08:30 | 2.01 | 15.62 | 10.625 | 10.000 | 12.125 | 11.500 | 11.532 | 23.143 |
| 05/11 08:15 | 05/11 08:05 | 0.96 | 16.58 | 10.563 | 10.563 | 12.063 | 12.063 | 12.094 | 11.632 |
| 05/14 08:37 | 05/14 08:25 | 3.01 | 19.58 | 10.438 | 10.438 | 11.938 | 11.938 | 12.001 | 36.085 |
| 05/16 08:55 | 05/16 08:45 | 2.01 | 21.59 | 10.313 | 10.313 | 11.813 | 11.813 | 11.876 | 23.817 |

| TABLE A2: TIME-AVERAGED HEAD IN THE OUTER RING | | | | | | | | | |
|---|---|---|---|---|---|---|---|---|---|
| Date/ Time On | Date/ Time Off | Δt (day) | Σt (day) | H On (in) | H Off (in) | Corr. H On (in) | Corr. H Off (in) | Av. H (in) | Weighted H (in-d) |
| 05/20 07:48 | 05/20 07:43 | 3.95 | 25.54 | 10.188 | 10.188 | 11.688 | 11.688 | 11.751 | 46.414 |
| 05/23 08:18 | 05/23 08:10 | 3.02 | 28.55 | 10.063 | 10.063 | 11.563 | 11.563 | 11.626 | 35.054 |
| 05/27 09:08 | 05/27 08:16 | 4.00 | 32.55 | 10.500 | 9.875 | 12.000 | 11.375 | 11.469 | 45.860 |
| 05/31 09:39 | 05/31 09:08 | 4.00 | 36.55 | 10.250 | 10.250 | 11.750 | 11.750 | 11.875 | 47.500 |
| 06/02 08:47 | 06/02 08:35 | 1.96 | 38.51 | 10.250 | 10.250 | 11.750 | 11.750 | 11.750 | 22.978 |
| 06/06 09:17 | 06/06 08:52 | 4.00 | 42.51 | 10.500 | 10.063 | 12.000 | 11.563 | 11.657 | 46.666 |
| 06/14 09:32 | 06/14 09:02 | 7.99 | 50.50 | 10.625 | 10.125 | 12.125 | 11.625 | 11.813 | 94.377 |
| 06/16 09:40 | 06/16 08:32 | 1.96 | 52.46 | 10.500 | 10.500 | 12.000 | 12.000 | 12.063 | 23.622 |

| TABLE A2: TIME-AVERAGED HEAD IN THE OUTER RING | | | | | | | | | |
|---|---|---|---|---|---|---|---|---|---|
| Date/ Time On | Date/ Time Off | Δt (day) | Σt (day) | H On (in) | H Off (in) | Corr. H On (in) | Corr. H Off (in) | Av. H (in) | Weighted H (in-d) |
| 06/22 09:28 | 06/22 08:18 | 5.94 | 58.40 | 10.375 | 10.250 | 11.875 | 11.750 | 11.875 | 70.574 |
| 06/30 09:18 | 06/30 08:15 | 7.95 | 66.35 | 10.625 | 9.875 | 12.125 | 11.375 | 11.625 | 92.411 |
| ----- ----- | 07/09 07:30 | 8.93 | 75.28 | ----- | 10.250 | ----- | 11.750 | 11.938 | 106.542 |
| | | | | Weighted Av. | | (in) | | | 11.786 |
| | | | | Weighted Av. | | (cm) | | | 29.94 |
| Scale on outer ring offset by 1.5"; Corrected Head = Head + 1.5" | | | | | | | | | |

Equation for Table A2

$$time\ averaged\ head = \frac{\Sigma(average\ depth\ for\ time\ interval * time\ interval)}{total\ time}$$

| TABLE A3: INFILTRATION RATE CALCULATIONS | | | | | | | | | | |
|---|---|---|---|---|---|---|---|---|---|---|
| Date/ Time On | Date/ Time Off | Δt (sec) | Σt (day) | Av. Temp (°F) | Av. Temp (°C) | Wt. On (g) | Wt. Off (g) | Flow (g) | Corr. Flow (ml) | Infil. Rate (cm/sec) |
| 04/24 15:35 | ----- ----- | ----- | ----- | --- | ---- | 1741 | ---- | ----- | ----- | ------- |
| 04/25 10:31 | 04/25 10:05 | 66600 | 0.77 | 76 | 24.4 | 1712 | 293 | 1448 | 1438 | 9.30e-07 |
| 04/26 09:26 | 04/26 09:10 | 81540 | 1.71 | 72 | 21.9 | 1601 | 553 | 1159 | 1153 | 6.09e-07 |
| 04/27 08:37 | 04/27 08:19 | 82380 | 2.67 | 69 | 20.6 | 1924 | 791 | 810 | 807 | 4.22e-07 |
| 04/28 08:23 | 04/28 08:19 | 85320 | 3.66 | 68 | 20.0 | 1475 | 1475 | 449 | 447 | 2.26e-07 |
| 04/29 08:40 | 04/29 08:30 | 86820 | 4.66 | 67 | 19.4 | 1729 | 1051 | 424 | 423 | 2.10e-07 |
| 04/30 08:27 | 04/30 08:15 | 84900 | 5.64 | 68 | 20.0 | 1414 | 1414 | 315 | 314 | 1.59e-07 |
| 05/01 08:21 | 05/01 08:11 | 85440 | 6.63 | 68 | 20.0 | 1920 | 1192 | 222 | 221 | 1.11e-07 |
| 05/02 07:55 | 05/02 07:50 | 84540 | 7.61 | 68 | 20.0 | 1738 | 1738 | 182 | 181 | 9.24e-08 |

| TABLE A3: INFILTRATION RATE CALCULATIONS | | | | | | | | | | |
|---|---|---|---|---|---|---|---|---|---|---|
| Date/ Time On | Date/ Time Off | Δt (sec) | Σt (day) | Av. Temp (°F) | Av. Temp (°C) | Wt. On (g) | Wt. Off (g) | Flow (g) | Corr. Flow (ml) | Infil. Rate (cm/sec) |
| 05/03 08:48 | 05/03 08:40 | 89100 | 8.64 | 67 | 19.4 | 1759 | 1556 | 182 | 181 | 8.77e-08 |
| 05/06 07:48 | 05/06 07:38 | 255000 | 11.59 | 67 | 19.4 | 1822 | 1266 | 493 | 491 | 8.30e-08 |
| 05/08 08:20 | 05/08 08:11 | 174180 | 13.61 | 69 | 20.6 | 1459 | 1459 | 363 | 362 | 8.94e-08 |
| 05/11 08:15 | 05/11 08:05 | 258300 | 16.60 | 70 | 21.1 | 2090 | 1232 | 227 | 226 | 3.77e-08 |
| 05/14 08:37 | 05/14 08:25 | 259800 | 19.61 | 70 | 21.1 | 1976 | 1793 | 297 | 296 | 4.90e-08 |
| 05/16 08:55 | 05/16 08:45 | 173280 | 21.61 | 70 | 21.1 | 2008 | 1817 | 159 | 158 | 3.93e-08 |
| 05/20 07:48 | 05/20 07:43 | 341280 | 25.56 | 71 | 21.7 | 1741 | 1741 | 267 | 266 | 3.35e-08 |
| 05/23 08:18 | 05/23 08:10 | 260520 | 28.58 | 72 | 22.2 | 1849 | 1565 | 176 | 175 | 2.89e-08 |

| TABLE A3: INFILTRATION RATE CALCULATIONS | | | | | | | | | | |
|---|---|---|---|---|---|---|---|---|---|---|
| Date/ Time On | Date/ Time Off | Δt (sec) | Σt (day) | Av. Temp (°F) | Av. Temp (°C) | Wt. On (g) | Wt. Off (g) | Flow (g) | Corr. Flow (ml) | Infil. Rate (cm/sec) |
| 05/27 09:08 | 05/27 08:16 | 345480 | 32.58 | 74 | 23.3 | 1943 | 1731 | 118 | 117 | 1.46e-08 |
| 05/31 09:39 | 05/31 09:08 | 345600 | 36.58 | 74 | 23.3 | 2002 | 2055 | -112 | -111 | -1.39e-08 |
| 06/02 08:47 | 06/02 08:35 | 168960 | 38.53 | 72 | 22.2 | 2008 | 1769 | 233 | 232 | 5.91e-08 |
| 06/06 09:17 | 06/06 08:52 | 345900 | 42.53 | 73 | 22.8 | 2046 | 1837 | 171 | 170 | 2.12e-08 |
| 06/14 09:32 | 06/14 09:02 | 690300 | 50.52 | 75 | 23.9 | 2236 | 2236 | -190 | -189 | -1.18e-08 |
| 06/16 09:40 | 06/16 08:32 | 169200 | 52.48 | 77 | 25.0 | 2136 | 2136 | 100 | 99 | 2.53e-08 |
| 06/22 09:28 | 06/22 08:18 | 513480 | 58.43 | 79 | 26.1 | 2375 | 2375 | -239 | -237 | -1.99e-08 |
| 06/30 09:18 | 06/30 08:15 | 686820 | 66.37 | 81 | 27.2 | 2575 | 2575 | -200 | -198 | -1.24e-08 |

| TABLE A3: INFILTRATION RATE CALCULATIONS | | | | | | | | | | |
|---|---|---|---|---|---|---|---|---|---|---|
| Date/ Time On | Date/ Time Off | Δt (sec) | Σt (day) | Av. Temp (°F) | Av. Temp (°C) | Wt. On (g) | Wt. Off (g) | Flow (g) | Corr. Flow (ml) | Infil. Rate (cm/sec) |
| ----- | 07/09 07:30 | 771120 | 75.30 | 83 | 28.3 | ----- | 3250 | -675 | -667 | -3.73e-08 |

Equations for Table A3

$$Infiltration\ Rate = I = \frac{Q}{At}$$

$A = area\ of\ inner\ ring = 23{,}225.8\ cm^2$ $t = time = \text{sec}$

$$Q = \frac{weight\ on - weight\ off}{\rho} \qquad Q = cm^3 \qquad \rho = g/cm^3$$

$$\rho = 0.9998 + 7.1162x10^{-5}(T) - 9.2484x10^{-6}(T^2) + 7.5070x10^{-7}(T^3)$$

$$T(°C) = \left(\frac{5}{9}\right)(T(°F) - 32)$$

| TABLE A4: TDR VOLUMETRIC WATER CONTENT CALCULATIONS | | | | | | | |
|---|---|---|---|---|---|---|---|
| Profile #1 | | | | Profile #2 | | | |
| Depth (cm) | $L_{trace}$ (cm) | K | $\theta$ | Depth (cm) | $L_{trace}$ (cm) | K | $\theta$ |
| 1.5 | 18.4 | 13.82 | 0.26 | 2.0 | 18.8 | 14.42 | 0.27 |
| 3.0 | 18.0 | 13.22 | 0.25 | 6.6 | 18.2 | 13.52 | 0.25 |
| 4.0 | 17.6 | 12.64 | 0.24 | 7.5 | 18.0 | 13.22 | 0.25 |
| 6.5 | 16.6 | 11.25 | 0.21 | 9.5 | 18.6 | 14.12 | 0.26 |
| 10.5 | 17.4 | 12.36 | 0.23 | 12.5 | 18.0 | 13.22 | 0.25 |
| 14.0 | 17.4 | 12.36 | 0.23 | 14.5 | 19.6 | 15.68 | 0.29 |
| 16.5 | 18.6 | 14.12 | 0.26 | 17.0 | 19.0 | 14.73 | 0.27 |
| 18.5 | 17.6 | 12.64 | 0.24 | 19.5 | 19.2 | 15.04 | 0.28 |
| 21.0 | 19.4 | 15.36 | 0.28 | 21.0 | 18.6 | 14.12 | 0.26 |
| 22.0 | 19.6 | 15.68 | 0.29 | 25.0 | 18.8 | 14.42 | 0.27 |
| 23.0 | 19.6 | 15.68 | 0.29 | | | | |
| 25.0 | 19.0 | 14.73 | 0.27 | | | | |
| 27.5 | 19.4 | 15.36 | 0.28 | | | | |

| TABLE A4: TDR VOLUMETRIC WATER CONTENT CALCULATIONS | | | | | | | |
|---|---|---|---|---|---|---|---|
| Profile #3 | | | | Profile #4 | | | |
| Depth (cm) | $L_{trace}$ (cm) | K | $\theta$ | Depth (cm) | $L_{trace}$ (cm) | K | $\theta$ |
| 2.0 | 16.6 | 11.25 | 0.21 | 1.5 | 18.6 | 14.12 | 0.26 |
| 3.0 | 15.4 | 9.68 | 0.18 | 3.0 | 16.2 | 10.71 | 0.20 |
| 6.5 | 15.4 | 9.68 | 0.18 | 4.5 | 15.4 | 9.68 | 0.18 |
| 9.0 | 15.8 | 10.19 | 0.19 | 6.0 | 17.0 | 11.79 | 0.22 |
| 11.5 | 16.4 | 10.98 | 0.21 | 8.5 | 17.4 | 12.36 | 0.23 |
| 14.0 | 19.8 | 16.00 | 0.29 | 11.5 | 19.2 | 15.04 | 0.28 |
| 16.5 | 19.8 | 16.00 | 0.29 | 14.0 | 19.6 | 15.68 | 0.29 |
| 18.5 | 19.8 | 16.00 | 0.29 | 15.5 | 20.2 | 16.65 | 0.3 |
| 21.0 | 19.2 | 15.04 | 0.28 | 17.5 | 20.0 | 16.32 | 0.3 |
| 24.0 | 19.6 | 15.68 | 0.29 | 20.5 | 20.8 | 17.66 | 0.31 |
| | | | | 22.5 | 19.8 | 16.00 | 0.29 |
| | | | | 26.5 | 20.4 | 16.98 | 0.31 |

Equations for Table A4

$$K=\left(\frac{L_{trace}*multiplier}{L_{probe}}\right)^2$$

$$\theta_v=-5.3x10^{-2}+2.92x10^{-2}(K)-5.5x10^{-4}(K^2)+4.3x10^{-6}(K^3)$$

Tektronix TDR #1502B $L_{probe}$=15 cm
Probe spacing=2.5 cm Multiplier=0.33

| TABLE A5: Ion Chromatograph Bromide Data | | | | | | |
|---|---|---|---|---|---|---|
| Sample | Peak Height | Cal. Curve | IC $Br^-$ (mg/l) | Extract D.F. | IC D.F. | $Br^-$ (mg/l) |
| 1A-2 | 769 | 8 | 1.79 | 6.7 | 10 | 120 |
| 2A-2 | 745 | 8 | 1.73 | 6.7 | 10 | 116 |
| 3A-2 | 653 | 8 | 1.53 | 6.7 | 10 | 103 |
| 4A-2 | 524 | 8 | 1.25 | 6.7 | 10 | 84 |
| 1B-2 | 813 | 8 | 1.88 | 6.7 | 10 | 126 |
| 2B-2 | 707 | 8 | 1.65 | 6.7 | 10 | 111 |
| 3B-2 | 612 | 8 | 1.44 | 6.7 | 10 | 97 |
| 4B-2 | 505 | 8 | 1.21 | 6.7 | 10 | 81 |
| 1C-2 | 539 | 8 | 1.28 | 6.7 | 10 | 86 |
| 2C-2 | 476 | 8 | 1.14 | 6.7 | 10 | 77 |
| 3C-2 | 604 | 8 | 1.43 | 6.7 | 10 | 96 |
| 4C-2 | 522 | 8 | 1.25 | 6.7 | 10 | 84 |
| 1D-2 | 547 | 8 | 1.30 | 6.7 | 10 | 87 |
| 2D-2 | 363 | 8 | 0.90 | 6.7 | 10 | 60 |
| 3D-2 | 480 | 8 | 1.15 | 6.7 | 10 | 78 |
| 4D-2 | 557 | 8 | 1.32 | 6.7 | 10 | 89 |
| | | | | | | |
| 1A-4 | 3256 | 8 | 7.23 | 6.7 | 1 | 48 |
| 2A-4 | 2377 | 8 | 5.31 | 6.7 | 1 | 36 |
| 3A-4 | 3115 | 8 | 6.92 | 6.7 | 1 | 46 |
| 4A-4 | 2208 | 8 | 4.94 | 6.7 | 1 | 33 |
| 1B-4 | 3197 | 8 | 7.10 | 6.7 | 1 | 48 |
| 2B-4 | 2767 | 8 | 6.16 | 6.7 | 1 | 41 |

| TABLE A5: Ion Chromatograph Bromide Data | | | | | | |
|---|---|---|---|---|---|---|
| Sample | Peak Height | Cal. Curve | IC $Br^-$ (mg/l) | Extract D.F. | IC D.F. | $Br^-$ (mg/l) |
| 3B-4 | 3301 | 8 | 7.33 | 6.7 | 1 | 49 |
| 4B-4 | 2306 | 8 | 5.15 | 6.7 | 1 | 35 |
| 1C-4 | 2643 | 8 | 5.89 | 6.7 | 1 | 39 |
| 2C-4 | 2837 | 8 | 6.32 | 6.7 | 1 | 42 |
| 3C-4 | 2662 | 8 | 5.93 | 6.7 | 1 | 40 |
| 4C-4 | 2835 | 8 | 6.31 | 6.7 | 1 | 42 |
| 1D-4 | 2248 | 8 | 5.03 | 6.7 | 1 | 34 |
| 2D-4 | 3147 | 8 | 6.99 | 6.7 | 1 | 47 |
| 3D-4 | 2549 | 8 | 5.68 | 6.7 | 1 | 38 |
| 4D-4 | 3272 | 8 | 7.27 | 6.7 | 1 | 49 |
| | | | | | | |
| 1A-6 | 2955 | 6 | 6.20 | 6.7 | 1 | 42 |
| 2A-6 | 2851 | 6 | 5.99 | 6.7 | 1 | 40 |
| 3A-6 | 2813 | 6 | 5.91 | 6.7 | 1 | 40 |
| 4A-6 | 2448 | 6 | 5.15 | 6.7 | 1 | 35 |
| 1B-6 | 3053 | 6 | 6.41 | 6.7 | 1 | 43 |
| 2B-6 | 2557 | 6 | 5.38 | 6.7 | 1 | 36 |
| 3B-6 | 2674 | 6 | 5.62 | 6.7 | 1 | 38 |
| 4B-6 | 2251 | 6 | 4.75 | 6.7 | 1 | 32 |
| 1C-6 | 2333 | 6 | 4.92 | 6.7 | 1 | 33 |
| 2C-6 | 2498 | 6 | 5.26 | 6.7 | 1 | 35 |
| 3C-6 | 2153 | 6 | 4.54 | 6.7 | 1 | 30 |
| 4C-6 | 2024 | 6 | 4.28 | 6.7 | 1 | 29 |

| TABLE A5: Ion Chromatograph Bromide Data | | | | | | |
|---|---|---|---|---|---|---|
| Sample | Peak Height | Cal. Curve | IC $Br^-$ (mg/l) | Extract D.F. | IC D.F. | $Br^-$ (mg/l) |
| 1D-6 | 2312 | 6 | 4.87 | 6.7 | 1 | 33 |
| 2D-6 | 2228 | 6 | 4.70 | 6.7 | 1 | 32 |
| 3D-6 | 2387 | 6 | 5.03 | 6.7 | 1 | 34 |
| 4D-6 | 2515 | 6 | 5.29 | 6.7 | 1 | 35 |
| | | | | | | |
| 1A-8 | 1646 | 6 | 3.49 | 6.7 | 1 | 23 |
| 2A-8 | 1688 | 6 | 3.58 | 6.7 | 1 | 24 |
| 3A-8 | 1808 | 6 | 3.83 | 6.7 | 1 | 26 |
| 4A-8 | 1636 | 6 | 3.47 | 6.7 | 1 | 23 |
| 1B-8 | 1489 | 6 | 3.17 | 6.7 | 1 | 21 |
| 2B-8 | 1749 | 6 | 3.71 | 6.7 | 1 | 25 |
| 3B-8 | 1707 | 6 | 3.62 | 6.7 | 1 | 24 |
| 4B-8 | 2049 | 6 | 4.33 | 6.7 | 1 | 29 |
| 1C-8 | 2376 | 6 | 5.00 | 6.7 | 1 | 34 |
| 2C-8 | 1720 | 6 | 3.65 | 6.7 | 1 | 24 |
| 3C-8 | 1767 | 6 | 3.74 | 6.7 | 1 | 25 |
| 4C-8 | 1344 | 6 | 2.87 | 6.7 | 1 | 19 |
| 1D-8 | 2389 | 6 | 5.03 | 6.7 | 1 | 34 |
| 2D-8 | 2311 | 6 | 4.87 | 6.7 | 1 | 33 |
| 3D-8 | 2271 | 6 | 4.79 | 6.7 | 1 | 32 |
| 4D-8 | 2016 | 6 | 4.26 | 6.7 | 1 | 29 |
| | | | | | | |
| 1A-10 | 1961 | 7 | 3.58 | 6.7 | 1 | 24 |

| TABLE A5: Ion Chromatograph Bromide Data | | | | | | |
|---|---|---|---|---|---|---|
| Sample | Peak Height | Cal. Curve | IC $Br^-$ (mg/l) | Extract D.F. | IC D.F. | $Br^-$ (mg/l) |
| 2A-10 | 1451 | 4 | 2.65 | 6.7 | 1 | 18 |
| 3A-10 | 2035 | 4 | 3.70 | 6.7 | 1 | 25 |
| 4A-10 | 2004 | 7 | 3.66 | 6.7 | 1 | 25 |
| 1B-10 | 1533 | 3 | 2.53 | 6.7 | 1 | 17 |
| 2B-10 | 1661 | 4 | 3.03 | 6.7 | 1 | 20 |
| 3B-10 | 1795 | 4 | 3.27 | 6.7 | 1 | 22 |
| 4B-10 | 2192 | 4 | 3.98 | 6.7 | 1 | 27 |
| 1C-10 | 1872 | 4 | 3.41 | 6.7 | 1 | 23 |
| 2C-10 | 1775 | 7 | 3.25 | 6.7 | 1 | 22 |
| 3C-10 | 1549 | 7 | 2.84 | 6.7 | 1 | 19 |
| 4C-10 | 1024 | 8 | 2.34 | 6.7 | 1 | 16 |
| 1D-10 | 1960 | 8 | 4.39 | 6.7 | 1 | 29 |
| 2D-10 | 1549 | 7 | 2.84 | 6.7 | 1 | 19 |
| 3D-10 | 2019 | 7 | 3.68 | 6.7 | 1 | 25 |
| 4D-10 | 1222 | 7 | 2.25 | 6.7 | 1 | 15 |
| | | | | | | |
| 1A-12 | 1848 | 5 | 3.37 | 6.7 | 1 | 23 |
| 1B-12 | 1037 | 3 | 1.73 | 6.7 | 1 | 12 |
| 1C-12 | 1464 | 5 | 2.68 | 6.7 | 1 | 18 |
| 1D-12 | 2428 | 5 | 4.40 | 6.7 | 1 | 30 |
| 1A-14 | 1358 | 5 | 2.49 | 6.7 | 1 | 17 |
| 1B-14 | 892 | 3 | 1.50 | 6.7 | 1 | 10 |
| 1C-14 | 957 | 5 | 1.77 | 6.7 | 1 | 12 |

| TABLE A5: Ion Chromatograph Bromide Data | | | | | | |
|---|---|---|---|---|---|---|
| Sample | Peak Height | Cal. Curve | IC $Br^-$ (mg/l) | Extract D.F. | IC D.F. | $Br^-$ (mg/l) |
| 1D-14 | 1451 | 5 | 2.66 | 6.7 | 1 | 18 |
| 1A-16 | 1167 | 5 | 2.15 | 6.7 | 1 | 14 |
| 1B-16 | 739 | 3 | 1.26 | 6.7 | 1 | 8 |
| 1C-16 | 894 | 5 | 1.66 | 6.7 | 1 | 11 |
| 1D-16 | 861 | 5 | 1.60 | 6.7 | 1 | 11 |
| 1A-18 | 845 | 5 | 1.57 | 6.7 | 1 | 11 |
| 1B-18 | 637 | 3 | 1.09 | 6.7 | 1 | 7 |
| 1C-18 | 593 | 5 | 1.12 | 6.7 | 1 | 8 |
| 1D-18 | 645 | 5 | 1.21 | 6.7 | 1 | 8 |
| 1A-20 | 619 | 5 | 1.17 | 6.7 | 1 | 8 |
| 1B-20 | 421 | 3 | 0.74 | 6.7 | 1 | 5 |
| 1C-20 | 493 | 5 | 0.94 | 6.7 | 1 | 6 |
| 1D-20 | 481 | 5 | 0.92 | 6.7 | 1 | 6 |
| BK-1 | 123 | 3 | 0.26 | 6.7 | 1 | 2 |
| BK-2 | 171 | 3 | 0.34 | 6.7 | 1 | 2 |
| 7/09/91 OR | 3077 | 8 | 6.84 | 1 | 10 | 68 |
| 5/27/91 OR | 2992 | 8 | 6.65 | 1 | 10 | 67 |
| 6/30/91 OR | 3078 | 8 | 6.84 | 1 | 10 | 68 |
| 6/14/91 Bt | 2680 | 8 | 5.97 | 1 | 10 | 60 |

see Table A6 for Equations for Table A5

| TABLE A6: IC Calibration Curves | | | | |
|---|---|---|---|---|
| Date | Time | Curve No. | a | b |
| 4/5/92 | 22:29 | 1 | 0.02666 | 0.00179 |
| 4/5/92 | 00:21 | 2 | 0.03353 | 0.00176 |
| 4/5/92 | 19:02 | 3 | 0.06983 | 0.00161 |
| 4/7/92 | 00:34 | 4 | 0.06012 | 0.00179 |
| 4/7/92 | 18:33 | 5 | 0.06271 | 0.00179 |
| 4/15/92 | 04:03 | 6 | 0.09019 | 0.00207 |
| 4/8/92 | 04:51 | 7 | 0.05516 | 0.00180 |
| 4/18/92 | 00:55 | 8 | 0.10682 | 0.00219 |

Equations for Tables A5 and A6

$$IC\ Br^- = b(peak\ height) + a$$

$$Extract\ D.F. = \frac{volume\ of\ water\ added - volume\ water\ original}{volume\ water\ original}$$

$$volume\ water\ added\ (ml) = weight\ of\ air\ dry\ sample\ (g)$$

$$volume\ water\ original\ (ml) = weight\ water\ original\ (g) = (\theta)\ (weight\ of\ air\ dry\ sample\ (g))$$

$\rho_w = 1.0\ g/cm^3$ (*assumed*) $\theta = 0.13\ g/cm^3$ $\rho_d = 1.89\ g/cm^3$

| Table A7: Example Dilution Factor Calculations for 1A Profile | | | | | | | |
|---|---|---|---|---|---|---|---|
| Average Values from TDR Data | | | Extraction Information for 1A Profile | | | | |
| Depth (cm) | $\theta_v$ ($cm^3/cm^3$) | $\theta_g$ ($g/cm^3$) | Sample | Weight Clay (g) | Volume Water (ml) | Volume Milleq (ml) | D.F. |
| 2 | 0.233 | 0.123 | 1A-2 | 241.2 | 29.7 | 241 | 7.1 |
| 4 | 0.228 | 0.121 | 1A-4 | 242.8 | 29.3 | 243 | 7.3 |
| 6 | 0.220 | 0.116 | 1A-6 | 271.6 | 31.6 | 272 | 7.6 |
| 8 | 0.230 | 0.122 | 1A-8 | 258.1 | 31.4 | 258 | 7.2 |
| 10 | 0.235 | 0.124 | 1A-10 | 232.1 | 28.9 | 232 | 7.0 |
| 12 | 0.250 | 0.132 | 1A-12 | 168.6 | 22.3 | 169 | 6.6 |
| 14 | 0.260 | 0.138 | 1A-14 | 232.4 | 32.0 | 232 | 6.3 |
| 16 | 0.270 | 0.143 | 1A-16 | 216.3 | 30.9 | 216 | 6.0 |
| 18 | 0.275 | 0.146 | 1A-18 | 191.9 | 27.9 | 192 | 5.9 |
| 20 | 0.280 | 0.148 | 1A-20 | 239.6 | 35.5 | 240 | 5.8 |

see Tables A5 and A6 for Equations for Table A7

| Table A8: Example Error Analysis for Bromide Concentrations in Profile 1A (Constant vs. Variable Dilution Factor) | | | | | | | | | | |
|---|---|---|---|---|---|---|---|---|---|---|
| Sample | $Br^-$ Measurements from IC with ±0.1 mg/l Error | | | Back Calculated $Br^-$ Concentrations with Average D.F. | | | Back Calculated $Br^-$ Concentrations with Variable D.F. | | | Range mg/l |
| | $Br^-$ mg/l | +0.1 mg/l | -0.1 mg/l | $Br^-$ mg/l | +0.1 mg/l | -0.1 mg/l | $Br^-$ mg/l | +0.1 mg/l | -0.1 mg/l | |
| 1A-2 | 17.91 | 18.91 | 16.91 | 120.0 | 126.7 | 113.3 | 127.2 | 134.4 | 120.1 | 7.7 |
| 1A-4 | 7.237 | 7.337 | 7.137 | 48.5 | 49.2 | 47.8 | 52.8 | 53.5 | 52.1 | 4.3 |
| 1A-6 | 6.207 | 6.307 | 6.107 | 41.6 | 42.2 | 40.9 | 47.2 | 48.0 | 46.4 | 5.8 |
| 1A-8 | 3.497 | 3.597 | 3.397 | 23.4 | 24.1 | 22.8 | 25.2 | 25.9 | 24.5 | 1.8 |
| 1A-10 | 3.585 | 3.685 | 3.485 | 24.0 | 24.7 | 23.3 | 25.1 | 25.9 | 24.5 | 1.2 |
| 1A-12 | 3.371 | 3.471 | 3.271 | 22.6 | 23.3 | 21.9 | 22.2 | 22.8 | 21.5 | 0.5 |
| 1A-14 | 2.494 | 2.594 | 2.394 | 16.7 | 17.4 | 16.0 | 15.7 | 16.2 | 15.0 | 1.2 |
| 1A-16 | 2.152 | 2.252 | 2.052 | 14.4 | 15.1 | 13.7 | 12.9 | 13.5 | 12.3 | 1.6 |
| 1A-18 | 1.575 | 1.675 | 1.475 | 10.6 | 11.2 | 9.9 | 9.3 | 9.8 | 8.7 | 1.4 |
| 1A-20 | 1.171 | 1.271 | 1.071 | 7.8 | 8.5 | 7.2 | 6.8 | 7.3 | 6.2 | 1.2 |
| | | | | | | | | Average Range | | 2.7 |

Note that the IC Br- Concentration for Sample 1A-2 contains an extra dilution factor of 10 (used to bring the IC reading within the linear range of the calibration curve) and that the ±0.1 mg/l IC error thus becomes a ±1.0 mg/l.

Range=the difference between the values for +0.1 mg/l error with constant D.F. and +0.1 mg/l error with variable D.F., or the difference between the values for -0.1 mg/l error with constant D.F. and -0.1 mg/l error with variable D.F., whichever was greatest.

see Table A7 for Constant and Variable Dilution Factors
see Tables A5 and A6 for Additional Equations for Table A8

| Table A9: Theoretical Bromide Diffusion Profiles | | | | |
|---|---|---|---|---|
| Depth Below Wetting Front (cm) | Depth Below Wetting Front (m) | $\beta$ | erfc($\beta$) | Bromide (mg/l) |
| $D^* = 18.2 \times 10^{-10}$ $m^2/sec$ | | | | |
| 2 | 0.02 | 0.183798 | 0.79502 | 51 |
| 4 | 0.04 | 0.367595 | 0.60337 | 39 |
| 6 | 0.06 | 0.551393 | 0.43555 | 28 |
| 8 | 0.08 | 0.735191 | 0.29872 | 19 |
| 10 | 0.10 | 0.918988 | 0.19398 | 12 |
| 12 | 0.12 | 1.102786 | 0.11896 | 8 |
| 14 | 0.14 | 1.286584 | 0.06917 | 4 |
| 16 | 0.16 | 1.470381 | 0.03799 | 2 |
| 18 | 0.18 | 1.654179 | 0.02334 | 1 |
| 20 | 0.20 | 1.837976 | 0.00950 | 1 |

| Table A9: Theoretical Bromide Diffusion Profiles | | | | |
|---|---|---|---|---|
| Depth Below Wetting Front (cm) | Depth Below Wetting Front (m) | $\beta$ | erfc($\beta$) | Bromide (mg/l) |
| $D^* = 21 \times 10^{-10}$ $m^2/sec$ | | | | |
| 2 | 0.02 | 0.171106 | 0.80891 | 52 |
| 4 | 0.04 | 0.342213 | 0.62852 | 40 |
| 6 | 0.06 | 0.513319 | 0.46809 | 30 |
| 8 | 0.08 | 0.684425 | 0.33334 | 21 |
| 10 | 0.10 | 0.855531 | 0.22642 | 14 |
| 12 | 0.12 | 1.026638 | 0.14731 | 9 |
| 14 | 0.14 | 1.197744 | 0.09037 | 6 |
| 16 | 0.16 | 1.368850 | 0.05341 | 3 |
| 18 | 0.18 | 1.539957 | 0.02980 | 2 |
| 20 | 0.20 | 1.711063 | 0.01562 | 1 |

| Table A9: Theoretical Bromide Diffusion Profiles | | | | |
|---|---|---|---|---|
| Depth Below Wetting Front (cm) | Depth Below Wetting Front (m) | $\beta$ | erfc($\beta$) | Bromide (mg/l) |
| $D^* = 15.0 \times 10^{-10}$ m$^2$/sec | | | | |
| 2 | 0.02 | 0.202456 | 0.77466 | 50 |
| 4 | 0.04 | 0.404911 | 0.56698 | 36 |
| 6 | 0.06 | 0.607367 | 0.39052 | 25 |
| 8 | 0.08 | 0.809823 | 0.25229 | 16 |
| 10 | 0.10 | 1.012278 | 0.15269 | 10 |
| 12 | 0.12 | 1.214734 | 0.08620 | 6 |
| 14 | 0.14 | 1.417190 | 0.04534 | 3 |
| 16 | 0.16 | 1.619646 | 0.02219 | 1 |
| 18 | 0.18 | 1.822101 | 0.01009 | 1 |
| 20 | 0.20 | 2.024557 | 0.00426 | 0 |

Equations for Table A9

$$C_i(x,t) = C_o\, erfc(\beta) \qquad \beta = \frac{x}{2\sqrt{\theta_v D^* t}}$$

$t$=75.30 *days*=6,505,920sec $\qquad \theta_v$=0.26 $\qquad \frac{C_o}{C_i}$=64 *mg/l*

PICARD.FOR (written by Jim Yeh, Sept. 1991)

========== TRANSIENT SIMULATION ==========

---------- PICARD Iteration Scheme ----------

*** Parameters of Soil Properties Models***

| SOIL TYPE | KSAT | ALPHA | N | WCS | WCR | Ss |
|---|---|---|---|---|---|---|
| 1 ClayPa | 0.50000E-08 | 0.23800E-02 | 0.16888E+01 | 0.32370E+00 | 0.20400E+00 | 0.10000E-04 |

MODEL: van Genuchten

---------- SIMULATION PARAMETERS ----------

TOTAL NO. OF NODES= 21
DELZ= 1.000
DELT= 0.35000E-03
MINIMUM DELT = 0.10000E-09
TIME WEIGHTING FACTOR, EPS= 0.100
TIME STEP MULTIPLIER, XMULT = 1.100
MAXIMUM DELT, DELMAX = 0.18000E+05
TOLERANCE, TOL = 0.10000E+00
MAXIMUM NO. OF ITERATIONS, MAXIT = 25
FLOW = VERTICAL FLOW
ITERATION SCHEME = PICARD

```
          -------------------- ELEMENT SOIL TYPE INFORMATION --------------------
ELEM SOILELEM SOILELEM SOILELEM SOILELEM SOILELEM SOILELEM SOILELEM SOILELEM SOILELEM
SOIL
  1    1   2    1   3    1   4    1   5    1   6    1   7    1   8    1   9    1  10
 1
 11    1  12    1  13    1  14    1  15    1  16    1  17    1  18    1  19    1  20
 1

          ---------- INITIAL CONDITION ----------

-1200.00-1200.00-1200.00-1200.00-1200.00-1200.00-1200.00-1200.00-1200.00-1200.00
-1200.00-1200.00-1200.00-1200.00-1200.00-1200.00-1200.00-1200.00-1200.00-1200.00
-1200.00


           ------BOUNDARY CONDITIONS ------
           NODE TYPE     PSI         FLUX
              1    0     29.94  0.00000E+00
             21    0  -1200.00  0.00000E+00
```

SIMULATION RESULT AT TIME = 0.12960E+07

| Z | PSI | THETA |
|---|---|---|
| 0.20000E+02 | 0.29940E+02 | 0.32370E+00 |
| 0.19000E+02 | 0.33110E+01 | 0.32370E+00 |
| 0.18000E+02 | -0.27876E+02 | 0.32320E+00 |
| 0.17000E+02 | -0.72024E+02 | 0.32130E+00 |
| 0.16000E+02 | -0.13684E+03 | 0.31705E+00 |
| 0.15000E+02 | -0.24264E+03 | 0.30848E+00 |
| 0.14000E+02 | -0.44634E+03 | 0.29232E+00 |
| 0.13000E+02 | -0.86449E+03 | 0.26952E+00 |
| 0.12000E+02 | -0.11646E+04 | 0.25946E+00 |
| 0.11000E+02 | -0.11981E+04 | 0.25855E+00 |
| 0.10000E+02 | -0.11999E+04 | 0.25850E+00 |
| 0.90000E+01 | -0.12000E+04 | 0.25850E+00 |
| 0.80000E+01 | -0.12000E+04 | 0.25850E+00 |
| 0.70000E+01 | -0.12000E+04 | 0.25850E+00 |
| 0.60000E+01 | -0.12000E+04 | 0.25850E+00 |
| 0.50000E+01 | -0.12000E+04 | 0.25850E+00 |
| 0.40000E+01 | -0.12000E+04 | 0.25850E+00 |
| 0.30000E+01 | -0.12000E+04 | 0.25850E+00 |
| 0.20000E+01 | -0.12000E+04 | 0.25850E+00 |
| 0.10000E+01 | -0.12000E+04 | 0.25850E+00 |
| 0.00000E+00 | -0.12000E+04 | 0.25850E+00 |

* * * * MATERIAL BALANCE ERROR ANALYSIS * * * *

CULM. WATER IN = 0.3499E+00
CULM. WATER OUT = 0.1126E-02
CULM. WATER IN & OUT = 0.3487E+00
CULM. CHANGE IN STRG. = 0.3471E+00
CULM. WATER ERROR = 0.1617E-02
ERROR IN % (ERROR/CQNET*100) = 0.4635E+00

SIMULATION RESULT AT TIME = 0.25920E+07

| Z | PSI | THETA |
|---|---|---|
| 0.20000E+02 | 0.29940E+02 | 0.32370E+00 |
| 0.19000E+02 | 0.11436E+02 | 0.32370E+00 |
| 0.18000E+02 | -0.84232E+01 | 0.32363E+00 |
| 0.17000E+02 | -0.32455E+02 | 0.32306E+00 |
| 0.16000E+02 | -0.63200E+02 | 0.32176E+00 |
| 0.15000E+02 | -0.10337E+03 | 0.31941E+00 |
| 0.14000E+02 | -0.15844E+03 | 0.31540E+00 |
| 0.13000E+02 | -0.23990E+03 | 0.30871E+00 |
| 0.12000E+02 | -0.37434E+03 | 0.29770E+00 |
| 0.11000E+02 | -0.62146E+03 | 0.28114E+00 |
| 0.10000E+02 | -0.10023E+04 | 0.26444E+00 |
| 0.90000E+01 | -0.11764E+04 | 0.25913E+00 |
| 0.80000E+01 | -0.11981E+04 | 0.25855E+00 |
| 0.70000E+01 | -0.11999E+04 | 0.25850E+00 |
| 0.60000E+01 | -0.12000E+04 | 0.25850E+00 |
| 0.50000E+01 | -0.12000E+04 | 0.25850E+00 |
| 0.40000E+01 | -0.12000E+04 | 0.25850E+00 |
| 0.30000E+01 | -0.12000E+04 | 0.25850E+00 |
| 0.20000E+01 | -0.12000E+04 | 0.25850E+00 |
| 0.10000E+01 | -0.12000E+04 | 0.25850E+00 |
| 0.00000E+00 | -0.12000E+04 | 0.25850E+00 |

* * * * MATERIAL BALANCE ERROR ANALYSIS * * * *

CULM. WATER IN = 0.4976E+00
CULM. WATER OUT = 0.1175E-02
CULM. WATER IN & OUT = 0.4964E+00
CULM. CHANGE IN STRG. = 0.4947E+00
CULM. WATER ERROR = 0.1698E-02
ERROR IN % (ERROR/CQNET*100) = 0.3421E+00

SIMULATION RESULT AT TIME = 0.38880E+07

| Z | PSI | THETA |
|---|---|---|
| 0.20000E+02 | 0.29940E+02 | 0.32370E+00 |
| 0.19000E+02 | 0.15125E+02 | 0.32370E+00 |
| 0.18000E+02 | -0.13089E+01 | 0.32370E+00 |
| 0.17000E+02 | -0.17662E+02 | 0.32347E+00 |
| 0.16000E+02 | -0.39030E+02 | 0.32283E+00 |
| 0.15000E+02 | -0.65246E+02 | 0.32166E+00 |
| 0.14000E+02 | -0.97970E+02 | 0.31976E+00 |
| 0.13000E+02 | -0.14018E+03 | 0.31680E+00 |
| 0.12000E+02 | -0.19734E+03 | 0.31227E+00 |
| 0.11000E+02 | -0.28032E+03 | 0.30532E+00 |
| 0.10000E+02 | -0.41244E+03 | 0.29480E+00 |
| 0.90000E+01 | -0.64057E+03 | 0.28007E+00 |
| 0.80000E+01 | -0.97800E+03 | 0.26527E+00 |
| 0.70000E+01 | -0.11638E+04 | 0.25948E+00 |
| 0.60000E+01 | -0.11960E+04 | 0.25860E+00 |
| 0.50000E+01 | -0.11996E+04 | 0.25851E+00 |
| 0.40000E+01 | -0.12000E+04 | 0.25850E+00 |
| 0.30000E+01 | -0.12000E+04 | 0.25850E+00 |
| 0.20000E+01 | -0.12000E+04 | 0.25850E+00 |
| 0.10000E+01 | -0.12000E+04 | 0.25850E+00 |
| 0.00000E+00 | -0.12000E+04 | 0.25850E+00 |

* * * * MATERIAL BALANCE ERROR ANALYSIS * * * *

CULM. WATER IN = 0.6118E+00
CULM. WATER OUT = 0.1260E-02
CULM. WATER IN & OUT = 0.6105E+00
CULM. CHANGE IN STRG. = 0.6088E+00
CULM. WATER ERROR = 0.1743E-02
ERROR IN % (ERROR/CQNET*100) = 0.2855E+00

SIMULATION RESULT AT TIME = 0.51840E+07

| Z | PSI | THETA |
|---|---|---|
| 0.20000E+02 | 0.29940E+02 | 0.32370E+00 |
| 0.19000E+02 | 0.16799E+02 | 0.32370E+00 |
| 0.18000E+02 | 0.41891E+01 | 0.32370E+00 |
| 0.17000E+02 | -0.10142E+02 | 0.32361E+00 |
| 0.16000E+02 | -0.26804E+02 | 0.32324E+00 |
| 0.15000E+02 | -0.46721E+02 | 0.32252E+00 |
| 0.14000E+02 | -0.70580E+02 | 0.32138E+00 |
| 0.13000E+02 | -0.99661E+02 | 0.31965E+00 |
| 0.12000E+02 | -0.13605E+03 | 0.31711E+00 |
| 0.11000E+02 | -0.18329E+03 | 0.31342E+00 |
| 0.10000E+02 | -0.24783E+03 | 0.30805E+00 |
| 0.90000E+01 | -0.34233E+03 | 0.30023E+00 |
| 0.80000E+01 | -0.49249E+03 | 0.28911E+00 |
| 0.70000E+01 | -0.74011E+03 | 0.27498E+00 |
| 0.60000E+01 | -0.10409E+04 | 0.26316E+00 |
| 0.50000E+01 | -0.11730E+04 | 0.25923E+00 |
| 0.40000E+01 | -0.11965E+04 | 0.25859E+00 |
| 0.30000E+01 | -0.11996E+04 | 0.25851E+00 |
| 0.20000E+01 | -0.12000E+04 | 0.25850E+00 |
| 0.10000E+01 | -0.12000E+04 | 0.25850E+00 |
| 0.00000E+00 | -0.12000E+04 | 0.25850E+00 |

* * * * MATERIAL BALANCE ERROR ANALYSIS * * * *

CULM. WATER IN = 0.7090E+00
CULM. WATER OUT = 0.1603E-02
CULM. WATER IN & OUT = 0.7074E+00
CULM. CHANGE IN STRG. = 0.7058E+00
CULM. WATER ERROR = 0.1611E-02
ERROR IN % (ERROR/CQNET*100) = 0.2278E+00

SIMULATION RESULT AT TIME = 0.64800E+07

| Z | PSI | THETA |
|---|---|---|
| 0.20000E+02 | 0.29940E+02 | 0.32370E+00 |
| 0.19000E+02 | 0.18401E+02 | 0.32370E+00 |
| 0.18000E+02 | 0.27793E+01 | 0.32370E+00 |
| 0.17000E+02 | -0.13329E+01 | 0.32370E+00 |
| 0.16000E+02 | -0.20721E+02 | 0.32340E+00 |
| 0.15000E+02 | -0.35395E+02 | 0.32296E+00 |
| 0.14000E+02 | -0.54479E+02 | 0.32218E+00 |
| 0.13000E+02 | -0.77281E+02 | 0.32101E+00 |
| 0.12000E+02 | -0.10445E+03 | 0.31934E+00 |
| 0.11000E+02 | -0.13776E+03 | 0.31698E+00 |
| 0.10000E+02 | -0.17994E+03 | 0.31369E+00 |
| 0.90000E+01 | -0.23562E+03 | 0.30907E+00 |
| 0.80000E+01 | -0.31330E+03 | 0.30259E+00 |
| 0.70000E+01 | -0.42941E+03 | 0.29354E+00 |
| 0.60000E+01 | -0.61382E+03 | 0.28157E+00 |
| 0.50000E+01 | -0.88850E+03 | 0.26857E+00 |
| 0.40000E+01 | -0.11161E+04 | 0.26085E+00 |
| 0.30000E+01 | -0.11859E+04 | 0.25887E+00 |
| 0.20000E+01 | -0.11980E+04 | 0.25855E+00 |
| 0.10000E+01 | -0.11997E+04 | 0.25850E+00 |
| 0.00000E+00 | -0.12000E+04 | 0.25850E+00 |

* * * * MATERIAL BALANCE ERROR ANALYSIS * * * *

CULM. WATER IN = 0.7946E+00
CULM. WATER OUT = 0.1621E-02
CULM. WATER IN & OUT = 0.7929E+00
CULM. CHANGE IN STRG. = 0.7914E+00
CULM. WATER ERROR = 0.1590E-02
ERROR IN % (ERROR/CQNET*100) = 0.2006E+00

## REFERENCES

American Society for Testing and Materials, "Standard Test Methods for Moisture-Density Relations of Soils and Soil-Aggregate Mixtures Using 5.5-lb.(2.49-kg) Rammer and 12-in.(305-mm) Drop (D 698A)", Annual Book of ASTM Standards, Construction, Vol. 04.08, 1990, pp. 160-164.

American Society for Testing and Materials, "Standard Practice for Description and Identification of Soils (Visual-Manual Procedure) (D 2488)", Annual Book of ASTM Standards, Construction, Vol. 04.08, 1990, pp. 305-314.

American Society for Testing and Materials, "Standard Test for Liquid Limit, Plastic Limit, and Plasticity Index of Soils (D 4318)", Annual Book of ASTM Standards, Construction, Vol. 04.08, 1990, pp. 591-601.

American Society for Testing and Materials, "Standard Method for Particle-Size Analysis of Soils (D 422)", Annual Book of ASTM Standards, Construction, Vol. 04.08, 1990, pp. 91-97.

American Society for Testing and Materials, "Standard Test Method for Amount of Material in Soils Finer Than the No. 200 (75-$\mu$m) Sieve (D 1140)", Annual Book of ASTM Standards, Construction, Vol. 04.08, 1990, pp. 183-184.

Bailey, B.B., Geddis, A.M., Hsu, S.S., Norton, D., Whitaker, M., Detty, T., Guzman-Guzman, A., Johnejack, K., Correia de Simas, M., Young, M., and Sully, M.J., Page Ranch Site In-Situ Permeability Test - Test Plans, Hydrology 508, Vadose Zone Monitoring, Department of Hydrology and Water Resources, University of Arizona, Tucson, Arizona, March, 1991.

Bagchi, A., discussion of "Hydraulic Conductivity of Two Prototype Clay Liners" by S.R. Day and D.E. Daniel, Journal of Geotechnical Engineering, Vol. 112, No. 3, March, 1986, pp. 796-799.

Barraclough, P.B. and Tinker, P.B., "The Determination of Ionic Diffusion Coefficients In Field Soils I. Diffusion Coefficients in Sieved Soils in Relation to Water Content and Bulk Density", Journal of Soil Science, Vol. 32, 1981, pp. 225-236.

Barraclough, P.B. and Tinker, P.B., "The Determination of Ionic Diffusion Coefficients In Field Soils I. Diffusion of Bromide Ions in Undisturbed Soil Cores", Journal of Soil Science, Vol. 33, 1981, pp. 13-24.

Bowman, R.S., "Evaluation of Some New Tracers for Soil Water Studies, Soil Science Society of America Journal, Vol. 48, 1984, pp. 987-993.

Corey, J.C., "Evaluation of Dyes for Tracing Water Movement", Soil Science, Vol. 106, pp. 182-187.

Dakessian, S. and Lewis, L., discussion of "Hydraulic Conductivity of Two Prototype Clay Liners" by S.R. Day and D.E. Daniel, Journal of Geotechnical Engineering, Vol. 112, No. 3, March, 1986, pp. 799-801.

Daniel B. Stephens and Associates, Test Plans and Specifications for In-Situ Permeability Testing Program at the Weldon Springs Site, St. Charles County, Missouri, Alburquque, New Mexico, January, 1991.

Daniel, D.E., "Problems in Predicting the Permeability of Compacted Clay Liners", Symposium on Uranium Mill Tailings Management, Fort Collins, Colorado, 1981, pp. 665-675.

Daniel, D.E., "Predicting Hydraulic Conductivity of Clay Liners", Journal of Geotechnical Engineering, Vol. 110, No. 2, February, 1984, pp. 285-300.

Daniel, D.E., "In Situ Hydraulic Conductivity Tests for Compacted Clay", Journal of Geotechnical Engineering, Vol. 115, No. 9, September, 1989, pp. 1205-1226.

Daniel, D.E. and Trautwein, S.J., "Field Permeability Test for Earthen Liners", Use of In Situ Test in Geotechnical Engineering, Samuel P. Clemence, Editor, American Society of Civil Engineers, 1986, pp. 146-160.

Day, S.R. and Daniel, D.E., "Hydraulic Conductivity of Two Prototype Clay Liners", Journal of Geotechnical Engineering, Vol. 111, No. 8, August, 1985, pp. 957-970.

Drever, J.I., The Geochemistry of Natural Waters (second edition), Prentice-Hall, Inc., Englewood Cliffs, N.J., 1988, p. 91.

Elsbury, B.R., Daniel, D.E., Sraders, G.A., and Anderson, D.C., "Lessons Learned From Compacted Clay Liners", Journal of Geotechnical Engineering, Vol. 116, No. 11, November, 1990, pp. 1641-1660.

Freeze, R.A. and Cherry, J.A., Groundwater, Prentice-Hall, Inc., Englewood Cliffs, N.J., 1979.

Ghodrati, M. and Jury, W.A., "A Field Study Using Dyes to Characterize Preferential Flow of Water", Soil Science Society of America Journal, Vol. 54, 1990, pp. 1558-1563.

Hills, R.G., Wierenga, P.J., Hudson, D.B., and Kirkland, M.R., "The Second Las Cruces Trench Experiment: Experimental Results and Two-Dimensional Flow Predictions", Water Resources Research, Vol. 27, No. 10, October, 1991, pp. 2707-2718.

Holtz, R.D. and Kovacs, W.D., An Introduction to Geotechnical Engineering, Prentice-Hall, Inc., Englewood Cliffs, N.J., 1981, pp. 88-89.

Hussen, A.M., personal communication, Soil and Water Science Department, University of Arizona, Tucson, Arizona, 1992.

Johnson, R.L., Cherry, J.A., and Pankow, J.F., "Diffusive Contaminant Transport in Natural Clay: A Field Example and Implications for Clay-Lined Waste Disposal Sites", Environmental Science Technology, Vol. 23, No. 3, 1989, pp. 340-349.

Khaleel, R. and Yeh, T.C., "A Galerkin Finite Element Program for Simulating Unsaturated Flow in Porous Media", Ground Water, Vol. 23, No. 1, January-February 1985, pp. 90-96.

Olson, R.E. and Daniel, D.E., "Measurement of the Hydraulic Conductivity of Fine-Grained Soils", ASTM STP 746, 1981, pp. 18-64.

Pacey, J.G., Scharlin, R.J., discussion of "Hydraulic Conductivity of Two Prototype Clay Liners" by S.R. Day and D.E. Daniel, Journal of Geotechnical Engineering, Vol. 112, No. 3, March, 1986, pp. 806-808.

Panno, S.V., Herzog, B.L., Cartwright, K., Rehfeldt, K.R., Krapac, I.G., and Hensel, B.R., "Field-Scale Investigation of Infiltration Into a Compacted Soil Liner", Ground Water, Vol. 29, No. 6, November-December 1991, pp. 914-921.

Quigely, R.M., Yanful, E.K., and Fernandez, F., "Ion Transfer By Diffusion Through Clayey Barriers", Geotechnical Practice for Waste Disposal '87, Richard D. Woods, Editor, American Society of Civil Engineers, 1987, pp. 137-158.

Rogowski, A.S., "Hydraulic Conductivity of Compacted Clay Soils", 12th Annual EPA Symposium for Treatment and Land Disposal of Hazardous Waste, March, 1986, pp. 29-39.

Rowe, R.K., "Pollutant Transport Through Barriers", Geotechnical Practice for Waste Disposal '87, Richard D. Woods, Editor, American Society of Civil Engineers, 1987, pp. 159-181.

Rowe, R.K., Caers, C.J., and Barone, F., "Laboratory Determination of Diffusion and Distribution Coefficients of Contaminants Using Undisturbed Clayey Soil", Canadian Geotechnical Journal, Vol. 25, 1988, pp. 108-118.

Shackelford, C.D., Daniel, D.E., and Liljestrand, H.M., "Diffusion of Inorganic Chemical Species in Compacted Clay Soil", Journal of Contaminant Hydrology, Vol. 4, 1989, pp. 241-273.

Shackelford, C.D., "Laboratory Diffusion Testing for Waste Disposal-A Review", Journal of Contaminant Hydrology, Vol. 7, 1991, pp. 177-217.

Shackelford, C.D. and Daniel, D.E., "Diffusion in Saturated Soil. I: Background", Journal of Geotechnical Engineering, Vol. 117, No. 3, March, 1991, pp. 467-484.

Shackelford, C.D. and Daniel, D.E., "Diffusion in Saturated Soil. II: Results for Compacted Clay", Journal of Geotechnical Engineering, Vol. 117, No. 3, March, 1991, pp. 485-507.

Soil Science Society of America, Inc., Methods of Soil Analysis, Part 2, Chemical and Microbiological Properties (Second Edition), A.L. Page, Editor, pp. 168-170, 1982.

Topp, G.C., Davis, J.L., Annan, A.P., "Time Domain Reflectometry (TDR) and Its Application to Irrigation Scheduling", Advances in Irrigation, Vol. 3, 1985, pp. 107-127.

Trautwein, S., Installation and Operating Instructions for the Sealed Double Ring Infiltrometer, Trautwein Soil Testing Equipment, Houston, Texas, January, 1991.

Van Genuchten, M.Th., "A Closed-form Equation for Predicting the Hydraulic Conductivity of Unsaturated Soils", Soil Science Society of America Journal, Vol. 44, 1980, pp. 892-898.

U.S. EPA, Soil Properties, Classification, and Hydraulic Conductivity Testin, Draft Technical Resource Document for Public Comment (SW-925), Municipal Environmental Research Laboratory, Office of Research and Development, Cincinnati, Ohio, March, 1984, pp. 48-52.

U.S. Federal Register, Vol. 52, No. 103, May 29, 1987, pp. 20218-20311.